



Search for exotic decays of the Higgs boson into long-lived particles in pp collisions at $\sqrt{s} = 13$ TeV using displaced vertices in the ATLAS inner detector

The ATLAS Collaboration

A novel search for exotic decays of the Higgs boson into pairs of long-lived neutral particles, each decaying into a bottom quark pair, is performed using 139 fb^{-1} of $\sqrt{s} = 13$ TeV proton–proton collision data collected with the ATLAS detector at the LHC. Events consistent with the production of a Higgs boson in association with a leptonically decaying Z boson are analysed. Long-lived particle (LLP) decays are reconstructed from inner-detector tracks as displaced vertices with high mass and track multiplicity relative to Standard Model processes. The analysis selection requires the presence of at least two displaced vertices, effectively suppressing Standard Model backgrounds. The residual background contribution is estimated using a data-driven technique. No excess over Standard Model predictions is observed, and upper limits are set on the branching ratio of the Higgs boson to LLPs. Branching ratios above 10% are excluded at 95% confidence level for LLP mean proper lifetimes $c\tau$ as small as 4 mm and as large as 100 mm. For LLP masses below 40 GeV, these results represent the most stringent constraint in this lifetime regime.

Contents

1	Introduction	2
2	ATLAS detector	4
3	Data and simulated events	5
3.1	Signal simulation	5
3.2	Background simulation	6
4	Event reconstruction	6
4.1	Displaced vertices	8
5	Event selection	9
6	Background estimation	10
7	Signal systematic uncertainties	12
8	Results	14
9	Conclusion	16

1 Introduction

The discovery of a new particle consistent with the Higgs boson at the Large Hadron Collider in 2012 revealed the final missing piece of the Standard Model (SM) of particle physics [1, 2]. Since then, a physics programme has emerged which aims to scrutinize the properties of the Higgs boson and the nature of the Higgs sector. Assuming that new physics does not strengthen the couplings of the Higgs boson to W/Z bosons, current experimental constraints allow for branching ratios of the Higgs boson to visible beyond-the-SM (BSM) states of up to 21% [3, 4]. Further, many theories that aim to solve the shortcomings of the Standard Model point to the Higgs boson as a possible portal to new physics [5], with exotic Higgs boson decay modes being the primary phenomenological consequence and means of discovery [6–8].

Decays of the Higgs boson into particles with macroscopic mean proper lifetimes ($c\tau \gtrsim 100 \mu\text{m}$), known as long-lived particles (LLPs), are predicted by top-down theories and are further motivated by bottom-up considerations. Examples of top-down theories include those based on the concept of Neutral Naturalness, such as Folded SUSY [9, 10] and Quirky Little Higgs [11]. These models aim to solve the hierarchy problem by introducing quark partners that are not charged under the SM $SU(3)_C$ group, but instead under some new $SU(3)'$ gauge group [6]. While conventional solutions to the hierarchy problem with coloured quark partners, such as supersymmetry [12–17], are becoming increasingly constrained experimentally, the production cross section for such uncoloured quark partners is greatly reduced, easily evading experimental constraints while remaining discoverable at the LHC. If the quark partners are sufficiently heavy, pure- $SU(3)'$ glueballs ($SU(3)'$ -neutral bound states composed of $SU(3)'$ mediators) would lie at the bottom of the BSM particle mass spectrum. Glueball masses in the range 10–60 GeV are preferred theoretically, and could be produced in decays of the Higgs boson. At the bottom of the BSM mass spectrum, the only decay mode available to such glueballs would be to SM fermions through an

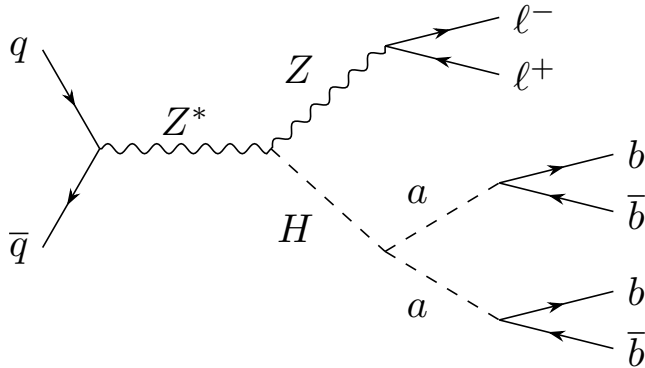


Figure 1: Tree-level Feynman diagram representing ZH production with $H \rightarrow aa \rightarrow b\bar{b}b\bar{b}$.

off-shell Higgs boson (with Yukawa-ordered branching ratios), causing decays into $b\bar{b}$ to dominate with lifetimes anywhere in the micrometer to kilometer range [6].

Bottom-up scenarios, such as hidden valleys [18, 19] and minimal scalar extensions to the SM, are also well motivated because the SM Higgs field admits the renormalizable portal interaction $\epsilon|S|^2H^\dagger H$. These simplified scenarios often arise naturally in the infrared limit of more complete theories such as Folded SUSY [9], and provide generic examples of scenarios in which the Higgs boson decays into LLPs.

This paper considers a simplified model in which a new electrically neutral pseudoscalar a boson is produced in pairs through decays of the Higgs boson, with the a boson subsequently decaying exclusively into $b\bar{b}$, as shown in Figure 1. The mean proper lifetime $c\tau_a$ and mass m_a of the a boson are treated as free parameters. Aside from the Haa interaction, the Higgs boson is assumed to be that of the SM.

Several searches for $H \rightarrow aa \rightarrow b\bar{b}b\bar{b}$ decays have been performed at the LHC, optimized for different regimes of $c\tau_a$. Searches based on standard b -tagging techniques were performed by ATLAS, with sensitivity for $c\tau_a \lesssim 1$ mm [20, 21]. While these searches focused on the topology of associated VH ($V = W, Z$) production of the Higgs boson, where leptonic V decays provide a trigger object, other searches have targeted gluon–gluon fusion production of the Higgs boson, which has a much larger cross section. For longer a boson lifetimes, standard b -tagging algorithms become inefficient compared to specialized reconstruction algorithms. The LHCb experiment performed a search for displaced vertices (DVs) resulting from LLP decays, obtaining sensitivity in the range $1 \text{ mm} \lesssim c\tau_a \lesssim 0.1 \text{ m}$ [22]. The CMS experiment also performed a DV-based search, yielding sensitivity in the range $1 \text{ mm} \lesssim c\tau_a \lesssim 1 \text{ m}$ for $m_a \geq 40 \text{ GeV}$ [23]. To identify LLP decays in the hadronic calorimeter, the ATLAS experiment selects jets that deposited anomalously more energy in the hadronic calorimeter than in the electromagnetic calorimeter (both at trigger level [24] and offline), providing sensitivity for $0.1 \text{ m} \lesssim c\tau_a \lesssim 10 \text{ m}$ [25]. Finally, ATLAS extends this sensitivity to $c\tau_a \lesssim 100 \text{ m}$ with searches for LLPs decaying within the muon spectrometer, by requiring a cluster of muon regions-of-interest from the first-level trigger [24] and a DV reconstructed from muon spectrometer tracklets [26, 27].

The search presented here targets LLP decays within the ATLAS inner-detector volume, resulting in the presence of at least two DVs that may be reconstructed from inner-detector tracks. The specialized algorithms for reconstruction of LLP decays are computationally expensive and therefore cannot be used at

trigger level or in the standard ATLAS reconstruction chain [28]. As a result, the ZH associated Higgs boson production topology is probed in this analysis, where $Z \rightarrow \ell\ell$ ($\ell = e, \mu$) decays provide highly efficient trigger objects. Based on the results of the standard event reconstruction, a small subset of the data is selected (as described in Section 5) for reprocessing with dedicated tracking and vertexing algorithms that can reconstruct displaced LLP decays [29, 30]. Finally, events are required to contain at least two DVs with high mass and track multiplicity relative to SM processes, effectively suppressing backgrounds. The residual background is estimated using a data-driven method and validated using an orthogonal signal-free data sample.

This is the first search for Higgs boson decays into LLPs to make use of this analysis methodology. Although it is assumed that the a boson is neutral and decays exclusively into $b\bar{b}$, these signal features are not explicitly exploited, so sensitivity is maintained for new physics scenarios with charged intermediate states and/or other hadronic decay modes. With this strategy, sensitivity to LLPs with $2 \text{ mm} \lesssim c\tau_a \lesssim 0.2 \text{ m}$ is obtained.

2 ATLAS detector

The ATLAS detector [31] at the LHC covers nearly the entire solid angle around the collision point.¹ It consists of an inner tracking detector surrounded by a thin superconducting solenoid, electromagnetic and hadron calorimeters, and a muon spectrometer incorporating three large superconducting air-core toroidal magnets.

The inner-detector system (ID) is immersed in a 2 T axial magnetic field and provides charged-particle tracking in the range $|\eta| < 2.5$. The high-granularity silicon pixel detector covers the vertex region and typically provides four measurements per track, the first hit normally being in the insertable B-layer installed before Run 2 [32, 33]. The geometry of the pixel detector consists of concentric barrel layers with $r = 33, 50.5, 88.5, \text{ and } 122.5 \text{ mm}$ in the central region, and three disks in each of the endcaps at $|z| = 495, 580, \text{ and } 650 \text{ mm}$. It is followed by the silicon microstrip tracker (SCT), consisting of barrel layers at $r = 299, 371, 443, \text{ and } 514 \text{ mm}$, spanning $|z| < 746 \text{ mm}$, and nine wheels in each of the endcaps with $854 < |z| < 2720 \text{ mm}$. The SCT usually provides eight measurements per track. These silicon detectors are complemented by the transition radiation tracker (TRT), which enables radially extended track reconstruction up to $|\eta| = 2.0$. The TRT also provides electron identification information based on the fraction of hits (typically 30 in total) above a higher energy-deposit threshold corresponding to transition radiation.

The calorimeter system covers the pseudorapidity range $|\eta| < 4.9$. Within the region $|\eta| < 3.2$, electromagnetic calorimetry is provided by barrel and endcap high-granularity lead/liquid-argon (LAr) calorimeters, with an additional thin LAr presampler covering $|\eta| < 1.8$ to correct for energy loss in material upstream of the calorimeters. Hadron calorimetry is provided by the steel/scintillator-tile calorimeter, segmented into three barrel structures within $|\eta| < 1.7$, and two copper/LAr hadron endcap calorimeters. The solid angle coverage is completed with forward copper/LAr and tungsten/LAr calorimeter modules optimized for electromagnetic and hadronic energy measurements respectively.

¹ ATLAS uses a right-handed coordinate system with its origin at the nominal interaction point (IP) in the centre of the detector and the z -axis along the beam pipe. The x -axis points from the IP to the centre of the LHC ring, and the y -axis points upwards. Cylindrical coordinates (r, ϕ) are used in the transverse plane, ϕ being the azimuthal angle around the z -axis. The pseudorapidity is defined in terms of the polar angle θ as $\eta = -\ln \tan(\theta/2)$. Angular distance is measured in units of $\Delta R \equiv \sqrt{(\Delta\eta)^2 + (\Delta\phi)^2}$.

The muon spectrometer (MS) comprises high-precision tracking chambers measuring the deflection of muons in a magnetic field generated by the superconducting air-core toroidal magnets. The field integral of the toroids ranges between 2.0 and 6.0 T m across most of the detector. A set of precision chambers covers the region $|\eta| < 2.7$ with three layers of monitored drift tubes, complemented by cathode-strip chambers in the forward region, where the background is highest. The muon trigger system covers the range $|\eta| < 2.4$ with resistive-plate chambers in the barrel, and thin-gap chambers in the endcap regions.

Interesting events are selected by the first-level trigger system implemented in custom hardware using information from the muon and calorimeter systems, followed by selections made by algorithms implemented in software in the high-level trigger [34]. The first-level trigger accepts events from the 40 MHz bunch crossings at a rate below 100 kHz, which the high-level trigger further reduces in order to record events to disk at about 1 kHz.

An extensive software suite [35] is used for real and simulated data reconstruction and analysis, for operation and in the trigger and data acquisition systems of the experiment.

3 Data and simulated events

This analysis uses 139.0 fb^{-1} of $\sqrt{s} = 13 \text{ TeV}$ pp collision data, collected by the ATLAS experiment from 2015 to 2018. Only data collected during stable beam conditions in which all detector subsystems were operational are considered [36]. Events were selected using the lowest unprescaled single-lepton (e, μ) triggers available during each data-taking year [37, 38]. Additional events selected with single-photon and diphoton triggers are used for validation of the background modelling strategy.

Simulated signal and background events were used to develop the analysis, optimize the event selection criteria, measure the signal selection efficiency, and assess sources of systematic uncertainty. The effect of multiple proton–proton interactions in the same or neighbouring bunches (pile-up) was modelled by overlaying the hard-scatter process with simulated inelastic proton–proton scattering events generated with PYTHIA 8.186 [39] using the NNPDF2.3lo PDF set [40] and the A3 set [41] of tuned parameters. The generated events were then run through a detailed GEANT4 [42] simulation of the ATLAS detector to simulate the detector response [43] and reconstructed using the same algorithms as used for the data.

3.1 Signal simulation

Samples of simulated events with a Higgs boson produced in association with a leptonically-decaying Z boson were generated using POWHEG BOX v2 [44–47]. The POWHEG BOX prediction is accurate to next-to-leading order (NLO) for $ZH + 1$ -jet production. Amplitudes for QCD virtual/loop corrections were constructed through the interface to the GoSAM package [48]. The loop-induced $gg \rightarrow ZH$ process was generated separately at leading order with POWHEG BOX. In all cases, the PDF4LHC15nlo PDF set [49] was used. The simulated samples are normalized to SM cross sections calculated at NNLO in QCD with NLO electroweak corrections for $q\bar{q} \rightarrow ZH$ and at NLO and next-to-leading-logarithm accuracy in QCD for $gg \rightarrow ZH$ [50–57], neglecting effects from potential Haa interactions.

The decay of the Higgs boson into two spin-0 a bosons and the subsequent decay of each a boson into a pair of b -quarks were simulated with PYTHIA 8.212 [39]. The coupling of the a boson to b -quarks is assumed to be that of a pseudoscalar; however, the analysis is insensitive to the parity of the a boson.

PYTHIA 8.212 was also used for parton showering and hadronization, as well as underlying-event simulation (using the AZNLO CTEQ6L1 set of tuned parameters [58]). Masses of the a boson in the range 16–55 GeV were considered, and statistically independent event samples were produced with $c\tau_a$ of 10 mm, 100 mm, and 1 m for each mass. These samples were reweighted to obtain samples corresponding to alternative lifetimes, where the weights were derived from the ratio of lifetime probability density functions.

The impact of using a different parton shower model on the p_T of the ZH system was evaluated by comparing the nominal $ZH, H \rightarrow aa$ samples with an additional sample produced with the POWHEG BOX v2 generator using the NNPDF3.0nnlo set of PDFs [59] and interfaced with HERWIG 7.2.1 [60, 61] using the H7.1-Default set of tuned parameters [62] and the MMHT2014nnlo PDF set [63].

3.2 Background simulation

While the background modeling strategy used in this analysis is fully data driven, simulated $Z + \text{jets}$ events are used to optimize the analysis selections and derive systematic uncertainties. The production of $Z + \text{jets}$ was simulated with the SHERPA 2.2.1 [64] generator using NLO matrix elements for up to two partons, and LO matrix elements for up to four partons calculated with the Comix [65] and OPENLOOPS 1 [66–68] libraries. They were matched with the SHERPA parton shower [69] using the MEPS@NLO prescription [70–73] using the set of tuned parameters developed by the SHERPA authors. The NNPDF3.0nnlo set of PDFs [59] was used.

4 Event reconstruction

Tracks are reconstructed from the collection of hits in the ID using a combinatorial Kalman filter [74]. The standard ATLAS track reconstruction algorithm is optimized for reconstruction of tracks that originate in the vicinity of the IP, and is not efficient for reconstructing displaced tracks corresponding to charged particles produced in LLP decays (although it is generally insensitive to the delayed arrival time of the decay products). To reconstruct these tracks, a secondary *large radius tracking* (LRT) algorithm is run on a subset of the data, taking as input the hits left over from the standard tracking procedure [29]. The LRT algorithm has looser requirements than the standard track reconstruction, particularly on the transverse and longitudinal impact parameters with respect to the primary vertex (d_0 and z_0). This algorithm is computationally expensive, but improves the overall reconstruction efficiency for hadrons produced at $r = 50$ (300) mm from about 20% (5%) to 90% (30%)². Hadrons produced with $r > 300$ mm traverse an insufficient number of tracker layers for reconstruction.

Events are required to contain a primary vertex (PV) associated with the pp hard scatter. The PV must have at least two tracks, each with $p_T > 500$ MeV. If more than one PV candidate satisfies these criteria, the candidate with the largest $\sum p_T^2$ is selected, where the sum extends over tracks associated with the vertex.

Electron candidates are reconstructed by matching clusters of energy in the calorimeters to reconstructed tracks [75]. Candidates are required to be within the fiducial region $|\eta| < 2.47$, and not within the calorimeter transition region ($1.37 < |\eta| < 1.52$). To reduce the background from non-prompt electrons and photon conversions, electrons must pass the Medium likelihood-based identification working point [75].

² The LRT reconstruction efficiency has a non-trivial dependence on track kinematics. The efficiencies quoted here were calculated from a simulated sample of LLP decays, yielding relatively-soft hadrons with p_T on the order of a few GeV [29].

Electron candidates are additionally required to have $|z_0 \sin \theta| < 0.5$ mm and $|d_0|/\sigma(d_0) < 5$, where $\sigma(d_0)$ is the uncertainty in the transverse impact parameter.

Photon candidates are similarly reconstructed from clusters of energy in the calorimeters. Candidates are required to have $|\eta| < 2.47$ and satisfy the Loose identification criteria [75].

Muon candidates are reconstructed from track segments in the muon spectrometer and matched to ID tracks [76, 77]. A combined track is then formed using the information from both detector subsystems. Candidates are required to pass the Medium reconstruction working point [77] and are further required to have $|\eta| < 2.5$, $|z_0 \sin \theta| < 0.5$ mm, and $|d_0|/\sigma(d_0) < 3$.

Hadronic jets are reconstructed from topological clusters [78] of energy deposits in the calorimeter, using the anti- k_t algorithm [79] with a radius parameter $R = 0.4$. Jets are calibrated using simulated events according to the procedure described in Refs. [80–84], followed by a residual calibration that takes into account the differences between data and simulation, and different detector response in the central ($|\eta| < 0.8$) versus forward ($|\eta| > 0.8$) region through the in situ calibration techniques described in Refs. [85, 86]. The jets considered in this analysis are required to have $p_T > 20$ GeV and $|\eta| < 2.5$.

The DL1 b -tagging algorithm quantifies the likelihood that a jet originated from a b -flavour quark versus a gluon g or light-flavour (u, d, s, c) quark [87, 88]. This algorithm exploits several features of b -jets, such as the lifetime, mass, and decay kinematics of b -hadrons, within a deep feed-forward neural network to distinguish between these hypotheses. Large values of the DL1 discriminant correspond to b -like jets.

Two additional track-based observables are used to discriminate between jets initiated by displaced partons resulting from LLP decays and those jets initiated by prompt partons. The first observable [89] exploits the fact that jets with modest displacement from the IP will contain tracks that are incompatible with all PV candidates. Each jet is assigned a vertex-fraction α_i to test its compatibility with PV candidate i ,

$$\alpha_i = p_T^{\text{trk}\epsilon i} / p_T^{\text{trk}},$$

where p_T^{trk} is the transverse component of the momentum of all tracks geometrically matched to the jet (using a shrinking cone algorithm) and $p_T^{\text{trk}\epsilon i}$ is defined similarly, but considering only the subset of tracks matched to primary vertex candidate i . A track is considered matched to a PV candidate if $|d_0| < 0.5$ mm and $|z_0 \sin \theta| < 0.3$ mm. A standard QCD jet should have a large value of α_i for the candidate PV at which it was produced, while jets originating from the decay of an LLP should have small values of α_i for all PV candidates. Therefore, the maximum α_i value for all PVs, $\alpha_{\text{max}} \equiv \max(\alpha_i)$, is used to discriminate between signal and QCD jets, as well as to reject jets originating from pile-up interactions.

The second observable exploits the fact that jets which are more significantly displaced deposit energy in the calorimeters but contain few reconstructed tracks. Therefore, the *charged hadron fraction* (f_{ch}) is defined as

$$f_{\text{ch}} = p_T^{\text{trk,prompt}} / p_T^{\text{jet}},$$

where $p_T^{\text{trk,prompt}}$ is the transverse component of the momentum of all tracks geometrically matched to the jet with $|d_0| < 0.5$ mm and p_T^{jet} is the jet transverse momentum.

Jets are considered “displaced” if they satisfy $\alpha_{\text{max}} < 0.05$ or $f_{\text{ch}} < 0.045$. This selection was optimized to provide high signal efficiency for a wide range of LLP proper lifetimes while maximizing background rejection.

4.1 Displaced vertices

Displaced vertices are reconstructed from the combined collection of standard and LRT tracks [30]. The algorithm proceeds in several steps. First, vertex reconstruction is seeded by pairs of tracks which were preselected with a series of quality criteria, including hit multiplicity requirements and $p_T > 1$ GeV. Further, at least one track must have $|d_0| > 2$ mm. The compatibility of each possible pair of preselected tracks is then assessed using the impact parameters of the tracks with respect to the estimated secondary vertex position, and those deemed loosely compatible are retained. The tracks are additionally required to pass a hit-pattern requirement which ensures that the hits associated with each track are compatible with a particle originating from the position of the seed vertex. These two-track seed vertices are then combined to form multi-track vertices. Nearby vertices are then merged, and tracks, including those that failed the preselection, are ultimately attached to compatible vertices provided that χ^2/n_{dof} of the updated vertex fit is less than 20. The efficiency of this vertex reconstruction is similar for light-flavour and heavy-flavour decays of the LLP, once its strong dependence on the multiplicity of charged LLP decay products is taken into account [30].

Reconstructed DVs are then pruned of tracks which are loosely associated with the vertex; only those tracks with a transverse (longitudinal) impact parameter with respect to the DV position satisfying $|d_0^{\text{DV}}| < 0.8$ mm ($|z_0^{\text{DV}}| < 1.2$ mm) with an uncertainty $\sigma(d_0^{\text{DV}}) < 0.1$ mm ($\sigma(z_0^{\text{DV}}) < 0.2$ mm) are retained. After track pruning, vertex properties are recalculated.

A vertex preselection is applied to reject low-quality fake DVs and those resulting from interactions between high-momentum hadrons and detector material. These interactions can produce a collimated spray of secondary hadrons, mimicking an LLP decay. Displaced vertices are required to fall within the geometric acceptance of the tracker, defined as $r < 300$ mm and $|z| < 300$ mm. DVs are further required to have $\chi^2/n_{\text{DoF}} < 5$. Finally, a *material veto* is applied to reject DVs whose position is compatible with the location of known detector elements [28].

Preselected DVs are dominated by the decay products of inelastic interactions between promptly produced particles and the detector material, and the decays of SM particles with significant lifetime. As shown in Figure 2, most of these DVs are rejected by requiring that the number of tracks associated with the vertex n_{trk} is greater than two. The remaining DVs result primarily from the random crossings of unrelated tracks in the vicinity of a metastable hadron decay. Particularly in the case of large crossing angles, these random crossings lead to artificially large values of the reconstructed vertex invariant mass. To identify such vertices, tracks associated with DVs are removed one-by-one and the angular separation ΔR between the momentum of the removed track and the combined momentum of the remaining vertex tracks is calculated, with the observable ΔR_{max} defined as the maximum of all such values. The *reduced mass* of the vertex is then calculated from the ratio of the reconstructed vertex invariant mass, m , and ΔR_{max} . As shown in Figure 2, the reduced mass discriminates strongly between signal and background DVs for all values of m_a probed. To reject vertices with random track crossings, DVs are required to have $m/\Delta R_{\text{max}} > 3$ GeV.

To reduce the background contribution from heavy-flavour hadron decays, additional cuts are placed on the significance of the vertex radial position measurement, defined as the ratio of the vertex radial position to its uncertainty $\sigma(r)$, and at least one track in the vertex must have $|d_0| > 3$ mm with respect to the PV. Finally, to facilitate the modelling of the background, a one-to-one matching between jets and DVs is performed, requiring DVs to be within $\Delta R = 0.6$ of one of the four leading jets. The full set of vertex selection criteria is shown in Table 1.

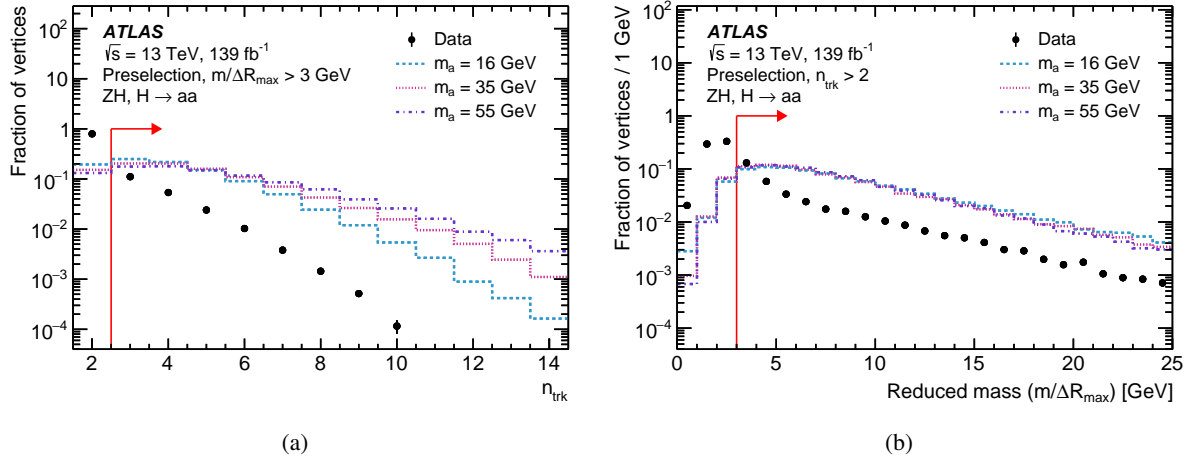


Figure 2: The distribution of (a) n_{trk} for preselected DVs with reduced mass exceeding 3 GeV and (b) reduced mass for preselected DVs with $n_{\text{trk}} > 2$, in simulated signal samples (dashed lines) and a background-enriched data sample (black points). DVs in events satisfying the control region selection, defined in Section 5, are considered. An arrow indicates the selection requirement which is applied to the observable. The distributions are normalized to unit area.

Table 1: The full set of selection criteria applied to DVs.

Selection type	Requirement
Track pruning	$ d_0^{\text{DV}} < 0.8 \text{ mm}$ $ z_0^{\text{DV}} < 1.2 \text{ mm}$ $\sigma(d_0^{\text{DV}}) < 0.1 \text{ mm}$ $\sigma(z_0^{\text{DV}}) < 0.2 \text{ mm}$
Vertex preselection	$\chi^2/n_{\text{DoF}} < 5$ $r < 300 \text{ mm}$ $ z < 300 \text{ mm}$ pass material veto
Vertex selection	$n_{\text{trk}} > 2$ $m/\Delta R_{\text{max}} > 3 \text{ GeV}$ $r/\sigma(r) > 100$ $\max(d_0) > 3 \text{ mm}$ $\Delta R_{\text{jet}} < 0.6$

5 Event selection

Events consistent with the $ZH, H \rightarrow aa$ topology were first selected using the lowest-threshold unprecaled single-lepton (e, μ) triggers operating during each data-taking year [37, 38]. Events are then identified for reprocessing with the LRT and displaced vertex reconstruction algorithms using an additional selection, referred to as a *filter*, which makes use of the results of the standard ATLAS reconstruction algorithms to identify jets consistent with originating from an LLP decay. The selection requires the presence of at least one jet with $p_{\text{T}} > 20 \text{ GeV}$, where at this stage the full jet calibration is not yet applied and the jet energy is calibrated at the electromagnetic scale [83]. At least one of the two leading, central ($|\eta| < 2.1$) jets must be

displaced. Finally, the filter requires the presence of a lepton from the Z boson decay. The number of events passing this filter is sufficiently small to permit reconstruction with the computationally expensive algorithms for displaced tracks and vertices. A second filter is also used, which selects events passing a high- p_T photon trigger, to facilitate the validation of the background estimation method.

After reconstruction with the LRT algorithm, the signal and control regions are defined by requiring events to contain two opposite-sign, same-flavour leptons. The leading (sub-leading) lepton is required to have $p_T > 27$ (10) GeV. To select events with a reconstructed Z boson, the dilepton invariant mass $m_{\ell\ell}$ is required to be in the range $66 < m_{\ell\ell} < 116$ GeV. Additionally, events are required to contain at least two jets. The trigger, filter, lepton, $m_{\ell\ell}$, and jet requirements comprise the event preselection. The signal region (SR) is then defined by requiring that events pass the preselection and contain at least two DVs passing the selections described in Section 4.1. To ensure robust modelling of the background, the DVs are required to be associated with different jets. Depending on the value of m_a , these criteria select ZH signal events with a leptonically-decaying Z boson with an efficiency ranging from 0.4% to 0.6% (0.04% to 0.2%) for $c\tau_a = 10$ (100) mm. A control region (CR) is defined similarly to the SR except for inversion of the DV multiplicity requirement, and is used to derive the background estimate. Despite the relatively low efficiency for signal events to satisfy the SR selection, signal contamination in the CR is negligible.

The background estimate is validated using an orthogonal γ +jet event selection. This *validation region* (VR) requires events to pass a high- p_T photon trigger, contain at least one photon with $p_T > 160$ GeV or two photons with $p_T > 60$ GeV, and at least two jets. Additionally, events containing charged leptons are vetoed in the VR to remove potential biases from signal. No requirement is placed on the number of displaced jets in the VR.

6 Background estimation

The probability for a jet to be matched to a DV within $\Delta R = 0.6$ is measured in the CR by taking the ratio of the number of jets matched to a DV to the total number of jets. This per-jet DV probability is observed to have a non-trivial dependence on the properties of the jet. The track multiplicity and density within a jet increase with the jet p_T [90], causing this probability to increase correspondingly. Due to the lifetime of hadrons containing heavy-flavour quarks, the probability also depends strongly on the flavour of the parton that initiated the jet. Therefore, the per-jet DV probability $P_{\text{DV}}(j)$ is parameterized as a function of jet p_T and DL1 b -tagging discriminant, as shown in Figure 3.

By restricting the computation of the per-jet DV probability to a region requiring fewer than two DVs, a bias of the order of P_{DV}^2 is introduced. However, due to the fact that $P_{\text{DV}} \ll 1$, these higher-order corrections are negligible.

The probability that an event contains a given number of DVs among the four leading jets may then be computed from a multinomial distribution. For example, the probability that an event contains exactly one DV is given by:

$$P_1 = \sum_{i=1}^4 P_{\text{DV}}(j_i) \times \prod_{k \neq i} (1 - P_{\text{DV}}(j_k)).$$

If the event contains fewer than four jets, then the probability is computed from all jets in the event. The probability for an event to fall in the SR is given by $P_{\geq 2} = 1 - P_0 - P_1$. Therefore, the background estimate is obtained by weighting preselected data events by $P_{\geq 2}$.

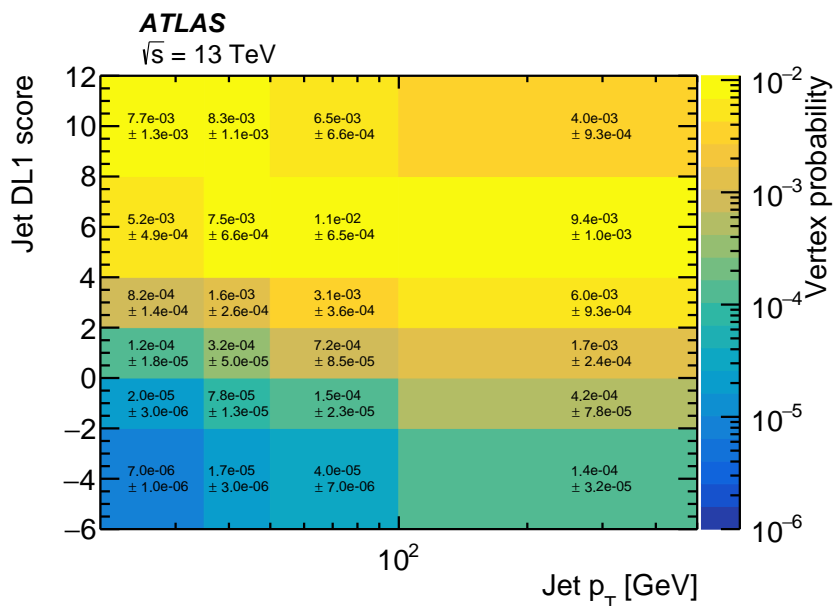


Figure 3: The per-jet DV probabilities computed in the CR, as a function of jet p_T and DL1 b -tag score. The rightmost column of bins is inclusive and includes jets with $p_T > 500$ GeV.

The presence of signal contamination in preselected data would increase the per-jet DV probability, as well as the population of events to which this probability is applied. Both of these effects would artificially increase the background estimate, potentially concealing the presence of signal in the SR. This effect was studied with a conservative assumption about the branching ratio $\mathcal{B}(H \rightarrow aa)$ and found to have less than a 10% effect on the background prediction, negligible in comparison to the size of injected signal.

To compute the uncertainty in the background estimate, pseudo-experiments are performed. Each pseudo-experiment is assigned a unique set of per-jet probabilities by varying each $(p_T, \text{DL1})$ bin within statistical uncertainties, and the varied probabilities are used to predict the background yield. The mean of the pseudo-experiments determines the central value of the expected yield, with its statistical uncertainty given by the RMS of pseudo-experiments. Using this method, a background estimate of 1.30 ± 0.08 events is obtained, where the uncertainty is statistical only.

This method for computing the background prediction relies on the assumption that the per-jet DV probabilities are unaffected by the presence of multiple DVs in an event. To validate this assumption, the VR defined in Section 5 is used. The parameterization of the per-jet DV probabilities in terms of p_T and DL1 allows for a robust validation of the method despite the kinematic properties of the jets in this region being different from those in the SR, and the absence of the displaced jet requirement leaves a statistically significant number of events to study. By comparing the predicted and observed numbers of events with at least two DVs in the VR, the core assumption of the background estimate may be tested and any systematic differences may be taken into account as an additional uncertainty in the background estimate.

Following the same procedure as is used in the CR, the per-jet DV probability is calculated using events in the VR with fewer than two DVs, and used to predict the number of events with at least two DVs. Using this method, a mean of 19.9 ± 0.4 events are predicted and 23 are observed, as shown in Figure 4, demonstrating that any jet–jet correlations are negligible or captured by the parameterization in terms of jet p_T and DL1.

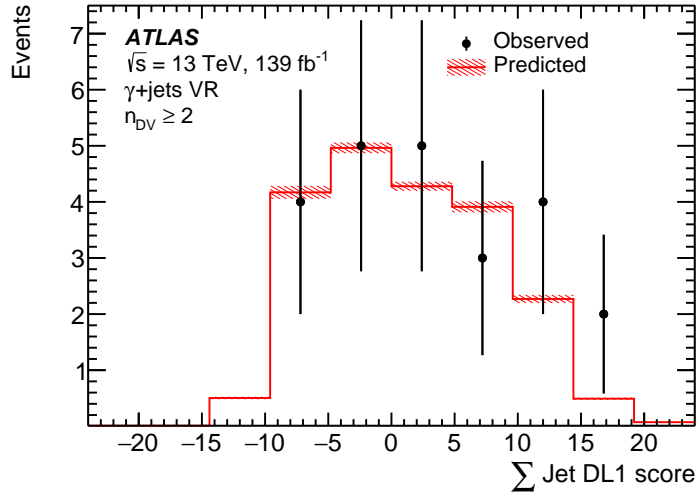


Figure 4: The predicted (solid line) and observed (black points) numbers of background events with at least two DVs in the γ +jet VR as a function of the sum of the DL1 b -tag scores of the (up to) four leading jets. The shaded band represents the statistical uncertainty of the prediction.

The systematic uncertainty of the method used to obtain the background prediction is derived by comparing the numbers of predicted and observed events in the VR. Although the prediction and observation agree within uncertainties, not many events are available to test the background estimation method. Consequently, a conservative systematic uncertainty, equal to the statistical uncertainty of the observed number of events in the VR, is assigned to the total expected number of background events in the SR. This amounts to a 21% uncertainty, or ± 0.27 events. This 21% uncertainty also covers the sensitivity of the background estimate to possible signal contamination impacting the per-jet DV probabilities, as discussed above.

Additional studies were performed by considering the subset of VR events that contain a displaced jet. This requirement reduces the statistical power of the VR, but makes it more representative of the SR. With the addition of this requirement, 2 events are observed compared to a prediction of 2.20 ± 0.10 (stat.), and the per-jet DV probabilities are compatible with those derived in the control region. This study provides further validation that the core assumptions of the background estimation method are robust against different event and object-level selections, but is ultimately not considered when deriving the systematic uncertainty on the background estimate due to the limited available statistics.

7 Signal systematic uncertainties

While the analysis is dominated by the statistical uncertainty of the observed data yield, several sources of experimental and theoretical uncertainty are considered that could potentially affect the signal efficiency.

Experimental uncertainties originating from differences between data and simulation are considered for all physics objects used in the analysis. For standard objects, these include uncertainties in the reconstruction and identification efficiencies, as well as the energy calibrations. Efficiency scale factors are used to correct the modelling of electrons and muons in simulation relative to data. These comprise electron identification and muon reconstruction scale factors as well as the scale factors applied to correct for trigger efficiency differences between data and simulation [37, 38, 75, 77]. The associated uncertainties are computed

by varying the scale factors up and down by one standard deviation and evaluating the impact on the final expected number of signal events. For jets, jet energy scale (JES) and jet energy resolution (JER) uncertainties are considered [91]. The applicability of the standard jet calibration scheme to the displaced jets considered in this analysis has been studied and found to be satisfactory [92]. Simulated events are reweighted such that the distribution of the average number of interactions per bunch crossing matches the distribution measured in data. Since the number of interactions per bunch crossing depends on the inelastic pp cross section, the difference between the predicted and measured cross sections [93] is propagated to the simulation by a systematic variation of the reweighted distribution.

The dominant systematic uncertainty in the expected signal yield originates from the non-standard reconstruction methods used. The uncertainty in the reconstruction of displaced vertices comes from the difference in performance of both the standard and LRT algorithms between data and simulation. For standard tracking, this uncertainty is known to be around 2% for tracks with small displacements from the IP [94]. To assess the uncertainty in the vertex reconstruction efficiency due to the modeling in the LRT algorithm, the rates of displaced vertices consistent with $K_S^0 \rightarrow \pi^+\pi^-$ decays are compared between data and Z+jets simulation. The uncertainty is estimated by examining the difference in K_S^0 yield between data and simulation. From the preselected events, candidate K_S^0 vertices are identified by requiring that the vertices pass the vertex preselection, have exactly two tracks of opposite charge, and have an invariant mass in the region 450 to 550 MeV. The simulation is normalized such that the number of K_S^0 vertices inside the beam pipe ($r < 23.5$ mm) is the same in data and simulation. This accounts for any K_S^0 decay yield differences that may exist between data and simulation in a region where tracking uncertainties are well understood. The p_T distributions of tracks from the K_S^0 vertices were found to be consistent between data and simulation. The vertex yields of K_S^0 are then compared between data and the normalized simulation in five bins of r ranging from zero to the radius of the last pixel layer (122 mm), beyond which there are significantly fewer vertices. The ratio quantifies the discrepancy between data and simulation in the number of K_S^0 vertices reconstructed from tracks outside of the beam pipe. To compute a per-track uncertainty, the square root of the ratio is taken because K_S^0 vertices are two-track vertices. This uncertainty is then added in quadrature with the 2% uncertainty from the standard tracking pass.

To propagate this uncertainty to the signal yield, tracks are randomly removed from reconstructed vertices in an uncorrelated fashion³ according to a uniform probability given by the per-track uncertainty corresponding to the r position of the vertex. The tracks are removed following the same track-pruning procedure as described in Section 4.1, and the vertex properties are recalculated from the updated set of associated tracks. The yield of vertices passing the full signal vertex selection is then compared between the modified and nominal vertex collections as a function of r , and the ratio of yields provides a scale factor corresponding to the reconstruction efficiency of each LLP. A per-event efficiency correction scale factor is obtained from the product of the scale factors corresponding to each LLP. The difference between the efficiency computed with the scale factors applied and the nominal selection efficiency is taken as the systematic uncertainty. This uncertainty is largest for small values of m_a and increases with the proper lifetime $c\tau_a$ to a maximum value of 12%.

Uncertainties associated with the displaced-jet filter are considered. The dominant contribution to the uncertainty originates from the use of uncalibrated jets in the filter. This uncertainty is estimated by raising the jet p_T threshold in the filter by 5 GeV, from 20 to 25 GeV, and calculating the change in filter efficiency on simulated signal samples. The choice of 5 GeV is motivated by studying the difference in efficiency of the uncalibrated jet p_T selection between data and simulation as a function of calibrated jet p_T .

³ A fully correlated method in which the entire vertex is removed was also investigated and gave similar results, but is believed to overestimate the uncertainty.

A theoretical uncertainty of $\pm 4\%$ and $\pm 25\%$ is assumed for the total $q\bar{q} \rightarrow ZH$ and $gg \rightarrow ZH, H \rightarrow aa$ cross section, respectively [50]. These uncertainties include effects from varying the factorization and renormalization scales, the PDF and α_s . To determine the uncertainty due to the choice of parton shower model, the nominal PYTHIA 8 samples are compared with a reference HERWIG 7 sample of ZH production. The p_T of the ZH system is compared between the two samples and used to reweight events in the PYTHIA signal samples to the reference HERWIG sample. The change in acceptance after reweighting is found to be of the order of 0.5% and is included as an additional systematic uncertainty in the signal modelling.

Finally, the expected number of signal events is subject to the uncertainty in the total integrated luminosity of the data sample used. The uncertainty in the combined 2015–2018 integrated luminosity is 1.7% [95], obtained using the LUCID-2 detector [96] for the primary luminosity measurements.

A summary of the systematic uncertainties is given in Table 2. With the exception of the uncertainties from the LRT algorithm and the displaced jet filter, the systematic uncertainties are not observed to vary significantly with m_a or $c\tau_a$ and are thus computed from the weighted average across samples.

Table 2: Summary of all sources of systematic uncertainty considered in the analysis that affect the signal yield. With the exception of the uncertainties from the filter and the LRT algorithm, no significant dependence on m_a or $c\tau_a$ is observed, so the quoted values are those derived from averaging over the different masses and lifetimes. The uncertainty from the filter efficiency was found to be uncorrelated with $c\tau_a$ but to increase with m_a , so the range quoted corresponds to the observed variation as m_a increases, after averaging over $c\tau_a$. The uncertainty from the LRT algorithm was found to be correlated with both $c\tau_a$ and m_a , so the quoted range corresponds to the observed variation with m_a and $c\tau_a$ (with the uncertainty increasing most strongly with $c\tau_a$).

Source	Uncertainty [%]
Theory	4.7
Luminosity	1.7
Pile-up reweighting	2.6
Electron identification	1.6
Electron calibration	0.4
Muon reconstruction	0.8
Muon calibration	0.4
Electron trigger	0.7
Muon trigger	1.3
Jet energy scale	1.4
Jet energy resolution	1.3
Filter	2.8–3.8
LRT	2.4–12
Total	7.4–14

8 Results

The mean number of background events predicted in the SR is 1.30 ± 0.08 (stat.) ± 0.27 (syst.). Zero events are observed in the signal region, compatible with the background prediction at the 68% confidence level (CL), as shown in Figure 5.

Upper limits at the 95% CL are set on the branching ratio of the Higgs boson to pairs of long-lived pseudoscalars $\mathcal{B}(H \rightarrow aa \rightarrow b\bar{b}b\bar{b})$ for each signal mass hypotheses, following the CL_s prescription [97]

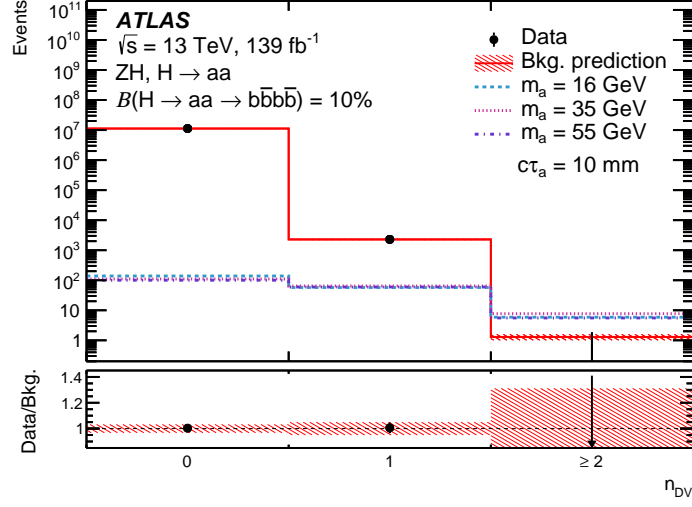


Figure 5: DV multiplicity among preselected events for signal (dashed lines), background prediction (solid line), and data (black points). The bins corresponding to $n_{DV} = 0$ and $n_{DV} = 1$ compose the CR, which is used to derive the background estimate. The third bin is the SR and contains all events with $n_{DV} \geq 2$. The shaded bands represent the combined statistical and systematic uncertainty of the prediction. Signal distributions are normalized assuming $\mathcal{B}(H \rightarrow aa \rightarrow b\bar{b}b\bar{b}) = 10\%$.

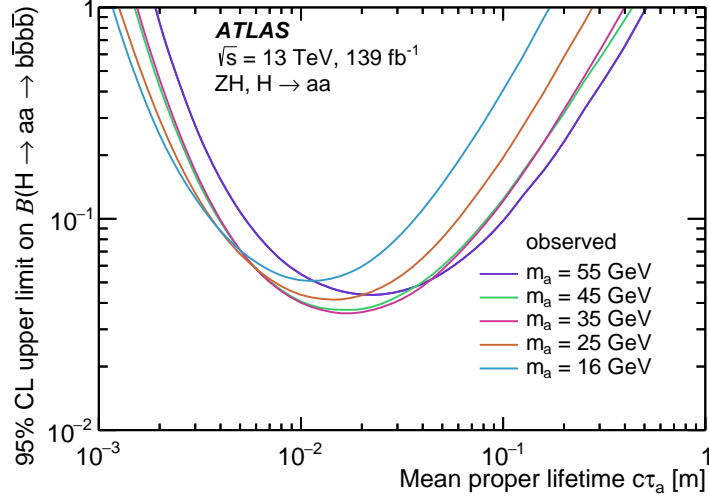


Figure 6: Observed 95% CL exclusion limits on $\mathcal{B}(H \rightarrow aa \rightarrow b\bar{b}b\bar{b})$ as a function of $c\tau_a$.

with a profile likelihood-ratio test statistic. A Poisson probability term describing the total number of observed events is used, with the systematic uncertainties of the signal and background yields treated as nuisance parameters and assigned Gaussian constraints with the appropriate widths, as described in Section 7. Pseudo-experiments which sample the distribution of the profile likelihood ratio are generated to compute the p -value and derive the exclusion limits. The observed limits for all signal mass points as a function of $c\tau_a$ are shown in Figure 6.

The limits are strongest for $c\tau_a \approx 10$ – 20 mm, probing values of $\mathcal{B}(H \rightarrow aa \rightarrow b\bar{b}b\bar{b})$ below $\sim 4\%$, and become weaker for shorter/longer lifetimes, primarily due to reduced radial acceptance. The limits depend

only weakly on the a boson mass, due to the relative insensitivity of the reduced-mass observable to m_a .

For $m_a = 16$ (55) GeV, a branching ratio greater than 10% is excluded at the 95% CL for $3.7 < c\tau_a < 37$ mm ($5.4 < c\tau_a < 102$ mm), probing an important gap in the ATLAS exotic Higgs decay programme. Decays of the Higgs boson into LLPs with shorter lifetimes are probed by conventional searches using standard b -tagging algorithms to identify signal events [20, 21], while decays into LLPs with longer lifetimes are probed by calorimeter- and MS-based searches utilizing dedicated LLP triggers [25–27].

9 Conclusion

A search for exotic decays of the Higgs boson into pairs of long-lived pseudoscalars (a) is presented, using 139 fb^{-1} of $\sqrt{s} = 13$ TeV pp collision data collected between 2015 and 2018 with the ATLAS experiment at the LHC. The search is performed in the topology of associated ZH production. Displaced vertices with high mass and track multiplicity relative to ones from SM processes are exploited as a signature of a boson decays and as a means to reject backgrounds. A data-driven method is used to assess the expected number of background events satisfying the event selection. The number of observed events is consistent with this prediction, and limits on the branching ratio $\mathcal{B}(H \rightarrow aa \rightarrow b\bar{b}b\bar{b})$ are calculated at the 95% CL. For masses below 40 GeV, these are the most stringent limits to date in the probed lifetime regime.

Acknowledgements

We thank CERN for the very successful operation of the LHC, as well as the support staff from our institutions without whom ATLAS could not be operated efficiently.

We acknowledge the support of ANPCyT, Argentina; YerPhI, Armenia; ARC, Australia; BMWFW and FWF, Austria; ANAS, Azerbaijan; SSTC, Belarus; CNPq and FAPESP, Brazil; NSERC, NRC and CFI, Canada; CERN; ANID, Chile; CAS, MOST and NSFC, China; Minciencias, Colombia; MSMT CR, MPO CR and VSC CR, Czech Republic; DNRF and DNSRC, Denmark; IN2P3-CNRS and CEA-DRF/IRFU, France; SRNSFG, Georgia; BMBF, HGF and MPG, Germany; GSRI, Greece; RGC and Hong Kong SAR, China; ISF and Benoziyo Center, Israel; INFN, Italy; MEXT and JSPS, Japan; CNRST, Morocco; NWO, Netherlands; RCN, Norway; MEiN, Poland; FCT, Portugal; MNE/IFA, Romania; JINR; MES of Russia and NRC KI, Russian Federation; MESTD, Serbia; MSSR, Slovakia; ARRS and MIZŠ, Slovenia; DSI/NRF, South Africa; MICINN, Spain; SRC and Wallenberg Foundation, Sweden; SERI, SNSF and Cantons of Bern and Geneva, Switzerland; MOST, Taiwan; TAEK, Turkey; STFC, United Kingdom; DOE and NSF, United States of America. In addition, individual groups and members have received support from BCKDF, CANARIE, Compute Canada and CRC, Canada; COST, ERC, ERDF, Horizon 2020 and Marie Skłodowska-Curie Actions, European Union; Investissements d’Avenir Labex, Investissements d’Avenir IDEX and ANR, France; DFG and AvH Foundation, Germany; Herakleitos, Thales and Aristeia programmes co-financed by EU-ESF and the Greek NSRF, Greece; BSF-NSF and GIF, Israel; Norwegian Financial Mechanism 2014-2021, Norway; NCN and NAWA, Poland; La Caixa Banking Foundation, CERCA Programme Generalitat de Catalunya and PROMETEO and GenT Programmes Generalitat Valenciana, Spain; Göran Gustafssons Stiftelse, Sweden; The Royal Society and Leverhulme Trust, United Kingdom.

The crucial computing support from all WLCG partners is acknowledged gratefully, in particular from CERN, the ATLAS Tier-1 facilities at TRIUMF (Canada), NDGF (Denmark, Norway, Sweden), CC-IN2P3

(France), KIT/GridKA (Germany), INFN-CNAF (Italy), NL-T1 (Netherlands), PIC (Spain), ASGC (Taiwan), RAL (UK) and BNL (USA), the Tier-2 facilities worldwide and large non-WLCG resource providers. Major contributors of computing resources are listed in Ref. [98].

References

- [1] ATLAS Collaboration, *Observation of a new particle in the search for the Standard Model Higgs boson with the ATLAS detector at the LHC*, *Phys. Lett. B* **716** (2012) 1, arXiv: [1207.7214 \[hep-ex\]](#).
- [2] CMS Collaboration, *Observation of a new boson at a mass of 125 GeV with the CMS experiment at the LHC*, *Phys. Lett. B* **716** (2012) 30, arXiv: [1207.7235 \[hep-ex\]](#).
- [3] ATLAS Collaboration, *Combined measurements of Higgs boson production and decay using up to 80 fb⁻¹ of proton–proton collision data at $\sqrt{s} = 13$ TeV collected with the ATLAS experiment*, *Phys. Rev. D* **101** (2020) 012002, arXiv: [1909.02845 \[hep-ex\]](#).
- [4] CMS Collaboration, *Combined measurements of Higgs boson couplings in proton–proton collisions at $\sqrt{s} = 13$ TeV*, *Eur. Phys. J. C* **79** (2019) 421, arXiv: [1809.10733 \[hep-ex\]](#).
- [5] B. Patt and F. Wilczek, *Higgs-field portal into hidden sectors*, (2006), arXiv: [hep-ph/0605188](#).
- [6] D. Curtin and C. B. Verhaaren, *Discovering Uncolored Naturalness in Exotic Higgs Decays*, *JHEP* **12** (2015) 072, arXiv: [1506.06141 \[hep-ph\]](#).
- [7] S. Bock et al., *Measuring hidden Higgs and strongly-interacting Higgs scenarios*, *Phys. Lett. B* **694** (2010) 44, arXiv: [1007.2645 \[hep-ph\]](#).
- [8] M. J. Strassler and K. M. Zurek, *Echoes of a hidden valley at hadron colliders*, *Phys. Lett. B* **651** (2007) 374, arXiv: [hep-ph/0604261 \[hep-ph\]](#).
- [9] G. Burdman, Z. Chacko, H.-S. Goh and R. Harnik, *Folded supersymmetry and the LEP paradox*, *JHEP* **02** (2007) 009, arXiv: [hep-ph/0609152 \[hep-ph\]](#).
- [10] T. Cohen, N. Craig, H. K. Lou and D. Pinner, *Folded supersymmetry with a twist*, *JHEP* **03** (2016) 196, arXiv: [1508.05396 \[hep-ph\]](#).
- [11] H. Cai, H.-C. Cheng and J. Terning, *A quirky little Higgs model*, *JHEP* **05** (2009) 045, arXiv: [0812.0843 \[hep-ph\]](#).
- [12] Y. A. Golfand and E. P. Likhtman, *Extension of the Algebra of Poincare Group Generators and Violation of p Invariance*, *JETP Lett.* **13** (1971) 323.
- [13] D. V. Volkov and V. P. Akulov, *Is the Neutrino a Goldstone Particle?*, *Phys. Lett. B* **46** (1973) 109.
- [14] J. Wess and B. Zumino, *Supergauge transformations in four dimensions*, *Nucl. Phys. B* **70** (1974) 39.
- [15] J. Wess and B. Zumino, *Supergauge invariant extension of quantum electrodynamics*, *Nucl. Phys. B* **78** (1974) 1.
- [16] S. Ferrara and B. Zumino, *Supergauge invariant Yang-Mills theories*, *Nucl. Phys. B* **79** (1974) 413.
- [17] A. Salam and J. Strathdee, *Super-symmetry and non-Abelian gauges*, *Phys. Lett. B* **51** (1974) 353.

- [18] M. J. Strassler, K. M. Zurek, *Discovering the Higgs through highly-displaced vertices*, *Phys. Lett. B* **661** (2008) 263, arXiv: [hep-ph/0605193](https://arxiv.org/abs/hep-ph/0605193) [[hep-ph](#)].
- [19] M. J. Strassler, K. Zurek, *Echoes of a hidden valley at hadron colliders*, *Phys. Lett. B* **651** (2007) 374, arXiv: [hep-ph/0604261](https://arxiv.org/abs/hep-ph/0604261).
- [20] ATLAS Collaboration, *Search for the Higgs boson produced in association with a vector boson and decaying into two spin-zero particles in the $H \rightarrow aa \rightarrow 4b$ channel in pp collisions at $\sqrt{s} = 13$ TeV with the ATLAS detector*, *JHEP* **10** (2018) 031, arXiv: [1806.07355](https://arxiv.org/abs/1806.07355) [[hep-ex](#)].
- [21] ATLAS Collaboration, *Search for Higgs boson decays into two new low-mass spin-0 particles in the $4b$ channel with the ATLAS detector using pp collisions at $\sqrt{s} = 13$ TeV*, *Phys. Rev. D* **102** (2020) 112006, arXiv: [2005.12236](https://arxiv.org/abs/2005.12236) [[hep-ex](#)].
- [22] LHCb Collaboration, *Updated search for long-lived particles decaying to jet pairs*, *Eur. Phys. J. C* **77** (2017) 812. 23 p.
- [23] CMS Collaboration, *Search for long-lived particles using displaced jets in proton-proton collisions at $\sqrt{s} = 13$ TeV*, (2020), arXiv: [2012.01581](https://arxiv.org/abs/2012.01581) [[hep-ex](#)].
- [24] ATLAS Collaboration, *Triggers for displaced decays of long-lived neutral particles in the ATLAS detector*, *JINST* **8** (2013) P07015, arXiv: [1305.2284](https://arxiv.org/abs/1305.2284) [[hep-ex](#)].
- [25] ATLAS Collaboration, *Search for long-lived neutral particles in pp collisions at $\sqrt{s} = 13$ TeV that decay into displaced hadronic jets in the ATLAS calorimeter*, *Eur. Phys. J. C* **79** (2019) 481, arXiv: [1902.03094](https://arxiv.org/abs/1902.03094) [[hep-ex](#)].
- [26] ATLAS Collaboration, *Search for long-lived particles produced in pp collisions at $\sqrt{s} = 13$ TeV that decay into displaced hadronic jets in the ATLAS muon spectrometer*, *Phys. Rev. D* **99** (2019) 052005, arXiv: [1811.07370](https://arxiv.org/abs/1811.07370) [[hep-ex](#)].
- [27] ATLAS Collaboration, *Search for long-lived neutral particles produced in pp collisions at $\sqrt{s} = 13$ TeV decaying into displaced hadronic jets in the ATLAS inner detector and muon spectrometer*, *Phys. Rev. D* **101** (2020) 052013, arXiv: [1911.12575](https://arxiv.org/abs/1911.12575) [[hep-ex](#)].
- [28] ATLAS Collaboration, *Search for long-lived, massive particles in events with displaced vertices and missing transverse momentum in $\sqrt{s} = 13$ TeV pp collisions with the ATLAS detector*, *Phys. Rev. D* **97** (2018) 052012, arXiv: [1710.04901](https://arxiv.org/abs/1710.04901) [[hep-ex](#)].
- [29] ATLAS Collaboration, *Performance of the reconstruction of large impact parameter tracks in the inner detector of ATLAS*, ATL-PHYS-PUB-2017-014, 2017, URL: <https://cds.cern.ch/record/2275635>.
- [30] ATLAS Collaboration, *Performance of vertex reconstruction algorithms for detection of new long-lived particle decays within the ATLAS inner detector*, ATL-PHYS-PUB-2019-013, 2019, URL: <https://cds.cern.ch/record/2669425>.
- [31] ATLAS Collaboration, *The ATLAS Experiment at the CERN Large Hadron Collider*, *JINST* **3** (2008) S08003.
- [32] ATLAS Collaboration, *ATLAS Insertable B-Layer: Technical Design Report*, ATLAS-TDR-19; CERN-LHCC-2010-013, 2010, URL: <https://cds.cern.ch/record/1291633>, Addendum: ATLAS-TDR-19-ADD-1; CERN-LHCC-2012-009, 2012, URL: <https://cds.cern.ch/record/1451888>.

- [33] B. Abbott et al., *Production and integration of the ATLAS Insertable B-Layer*, [JINST **13** \(2018\) T05008](#), arXiv: [1803.00844 \[physics.ins-det\]](#).
- [34] ATLAS Collaboration, *Performance of the ATLAS trigger system in 2015*, [Eur. Phys. J. C **77** \(2017\) 317](#), arXiv: [1611.09661 \[hep-ex\]](#).
- [35] ATLAS Collaboration, *The ATLAS Collaboration Software and Firmware*, ATL-SOFT-PUB-2021-001, 2021, URL: <https://cds.cern.ch/record/2767187>.
- [36] ATLAS Collaboration, *ATLAS data quality operations and performance for 2015–2018 data-taking*, [JINST **15** \(2020\) P04003](#), arXiv: [1911.04632 \[physics.ins-det\]](#).
- [37] ATLAS Collaboration, *Performance of electron and photon triggers in ATLAS during LHC Run 2*, [Eur. Phys. J. C **80** \(2020\) 47](#), arXiv: [1909.00761 \[hep-ex\]](#).
- [38] ATLAS Collaboration, *Performance of the ATLAS muon triggers in Run 2*, [JINST **15** \(2020\) P09015](#), arXiv: [2004.13447 \[hep-ex\]](#).
- [39] T. Sjöstrand et al., *An introduction to PYTHIA 8.2*, [Comput. Phys. Commun. **191** \(2015\) 159](#), arXiv: [1410.3012 \[hep-ph\]](#).
- [40] R. D. Ball et al., *Parton distributions with LHC data*, [Nucl. Phys. B **867** \(2013\) 244](#), arXiv: [1207.1303 \[hep-ph\]](#).
- [41] ATLAS Collaboration, *The Pythia 8 A3 tune description of ATLAS minimum bias and inelastic measurements incorporating the Donnachie–Landshoff diffractive model*, ATL-PHYS-PUB-2016-017, 2016, URL: <https://cds.cern.ch/record/2206965>.
- [42] GEANT4 Collaboration, S. Agostinelli et al., *GEANT4 – a simulation toolkit*, [Nucl. Instrum. Meth. A **506** \(2003\) 250](#).
- [43] ATLAS Collaboration, *The ATLAS Simulation Infrastructure*, [Eur. Phys. J. C **70** \(2010\) 823](#), arXiv: [1005.4568 \[physics.ins-det\]](#).
- [44] P. Nason and C. Oleari, *NLO Higgs boson production via vector-boson fusion matched with shower in POWHEG*, [JHEP **02** \(2010\) 037](#), arXiv: [0911.5299 \[hep-ph\]](#).
- [45] S. Alioli, P. Nason, C. Oleari and E. Re, *A general framework for implementing NLO calculations in shower Monte Carlo programs: the POWHEG BOX*, [JHEP **06** \(2010\) 043](#), arXiv: [1002.2581 \[hep-ph\]](#).
- [46] P. Nason, *A new method for combining NLO QCD with shower Monte Carlo algorithms*, [JHEP **11** \(2004\) 040](#), arXiv: [hep-ph/0409146](#).
- [47] S. Frixione, P. Nason and C. Oleari, *Matching NLO QCD computations with parton shower simulations: the POWHEG method*, [JHEP **11** \(2007\) 070](#), arXiv: [0709.2092 \[hep-ph\]](#).
- [48] G. Cullen et al., *Automated One-Loop Calculations with GoSam*, [Eur. Phys. J. C **72** \(2012\) 1889](#), arXiv: [1111.2034 \[hep-ph\]](#).
- [49] J. Butterworth et al., *PDF4LHC recommendations for LHC Run II*, [J. Phys. G **43** \(2016\) 023001](#), arXiv: [1510.03865 \[hep-ph\]](#).
- [50] D. de Florian et al., *Handbook of LHC Higgs Cross Sections: 4. Deciphering the Nature of the Higgs Sector*, (2016), arXiv: [1610.07922 \[hep-ph\]](#).

- [51] M. L. Ciccolini, S. Dittmaier and M. Krämer,
Electroweak radiative corrections to associated WH and ZH production at hadron colliders,
Phys. Rev. D **68** (2003) 073003, arXiv: [hep-ph/0306234](#) [[hep-ph](#)].
- [52] O. Brein, A. Djouadi and R. Harlander,
NNLO QCD corrections to the Higgs-strahlung processes at hadron colliders,
Phys. Lett. B **579** (2004) 149, arXiv: [hep-ph/0307206](#).
- [53] O. Brein, R. Harlander, M. Wiesemann and T. Zirke,
Top-Quark Mediated Effects in Hadronic Higgs-Strahlung, *Eur. Phys. J. C* **72** (2012) 1868,
arXiv: [1111.0761](#) [[hep-ph](#)].
- [54] L. Altenkamp, S. Dittmaier, R. V. Harlander, H. Rzehak and T. J. E. Zirke,
Gluon-induced Higgs-strahlung at next-to-leading order QCD, *JHEP* **02** (2013) 078,
arXiv: [1211.5015](#) [[hep-ph](#)].
- [55] A. Denner, S. Dittmaier, S. Kallweit and A. Mück, *HAWK 2.0: A Monte Carlo program for Higgs production in vector-boson fusion and Higgs strahlung at hadron colliders*,
Comput. Phys. Commun. **195** (2015) 161, arXiv: [1412.5390](#) [[hep-ph](#)].
- [56] O. Brein, R. V. Harlander and T. J. E. Zirke, *vh@nnlo – Higgs Strahlung at hadron colliders*,
Comput. Phys. Commun. **184** (2013) 998, arXiv: [1210.5347](#) [[hep-ph](#)].
- [57] R. V. Harlander, A. Kulesza, V. Theeuwes and T. Zirke,
Soft gluon resummation for gluon-induced Higgs Strahlung, *JHEP* **11** (2014) 082,
arXiv: [1410.0217](#) [[hep-ph](#)].
- [58] ATLAS Collaboration, *Measurement of the Z/ γ^* boson transverse momentum distribution in pp collisions at $\sqrt{s} = 7$ TeV with the ATLAS detector*, *JHEP* **09** (2014) 145,
arXiv: [1406.3660](#) [[hep-ex](#)].
- [59] R. D. Ball et al., *Parton distributions for the LHC run II*, *JHEP* **04** (2015) 040,
arXiv: [1410.8849](#) [[hep-ph](#)].
- [60] M. Bähr et al., *Herwig++ physics and manual*, *Eur. Phys. J. C* **58** (2008) 639,
arXiv: [0803.0883](#) [[hep-ph](#)].
- [61] J. Bellm et al., *Herwig 7.2 release note*, *Eur. Phys. J. C* **80** (2020) 452,
arXiv: [1912.06509](#) [[hep-ph](#)].
- [62] J. Bellm et al., *Herwig 7.1 Release Note*, (2017), arXiv: [1705.06919](#) [[hep-ph](#)].
- [63] L. Harland-Lang, A. Martin, P. Motylinski and R. Thorne,
Parton distributions in the LHC era: MMHT 2014 PDFs, *Eur. Phys. J. C* **75** (2015) 204,
arXiv: [1412.3989](#) [[hep-ph](#)].
- [64] E. Bothmann et al., *Event generation with Sherpa 2.2*, *SciPost Phys.* **7** (2019) 034,
arXiv: [1905.09127](#) [[hep-ph](#)].
- [65] T. Gleisberg and S. Höche, *Comix, a new matrix element generator*, *JHEP* **12** (2008) 039,
arXiv: [0808.3674](#) [[hep-ph](#)].
- [66] F. Buccioni et al., *OpenLoops 2*, *Eur. Phys. J. C* **79** (2019) 866, arXiv: [1907.13071](#) [[hep-ph](#)].
- [67] F. Cascioli, P. Maierhöfer and S. Pozzorini, *Scattering Amplitudes with Open Loops*,
Phys. Rev. Lett. **108** (2012) 111601, arXiv: [1111.5206](#) [[hep-ph](#)].

- [68] A. Denner, S. Dittmaier and L. Hofer,
COLLIER: A fortran-based complex one-loop library in extended regularizations,
Comput. Phys. Commun. **212** (2017) 220, arXiv: [1604.06792 \[hep-ph\]](#).
- [69] S. Schumann and F. Krauss,
A parton shower algorithm based on Catani–Seymour dipole factorisation, *JHEP* **03** (2008) 038,
arXiv: [0709.1027 \[hep-ph\]](#).
- [70] S. Höche, F. Krauss, M. Schönherr and F. Siegert,
A critical appraisal of NLO+PS matching methods, *JHEP* **09** (2012) 049,
arXiv: [1111.1220 \[hep-ph\]](#).
- [71] S. Höche, F. Krauss, M. Schönherr and F. Siegert,
QCD matrix elements + parton showers. The NLO case, *JHEP* **04** (2013) 027,
arXiv: [1207.5030 \[hep-ph\]](#).
- [72] S. Catani, F. Krauss, R. Kuhn and B. R. Webber, *QCD Matrix Elements + Parton Showers*,
JHEP **11** (2001) 063, arXiv: [hep-ph/0109231](#).
- [73] S. Höche, F. Krauss, S. Schumann and F. Siegert, *QCD matrix elements and truncated showers*,
JHEP **05** (2009) 053, arXiv: [0903.1219 \[hep-ph\]](#).
- [74] R. Frühwirth, *Application of Kalman filtering to track and vertex fitting*,
Nucl. Instrum. Methods **262** (1987) 444.
- [75] ATLAS Collaboration, *Electron and photon performance measurements with the ATLAS detector using the 2015–2017 LHC proton–proton collision data*, *JINST* **14** (2019) P12006,
arXiv: [1908.00005 \[hep-ex\]](#).
- [76] ATLAS Collaboration, *Muon reconstruction and identification efficiency in ATLAS using the full Run 2 pp collision data set at $\sqrt{s} = 13$ TeV*, (2020), arXiv: [2012.00578 \[hep-ex\]](#).
- [77] ATLAS Collaboration, *Muon reconstruction performance of the ATLAS detector in proton–proton collision data at $\sqrt{s} = 13$ TeV*, *Eur. Phys. J. C* **76** (2016) 292, arXiv: [1603.05598 \[hep-ex\]](#).
- [78] ATLAS Collaboration,
Topological cell clustering in the ATLAS calorimeters and its performance in LHC Run 1,
Eur. Phys. J. C **77** (2017) 490, arXiv: [1603.02934 \[hep-ex\]](#).
- [79] M. Cacciari, G. P. Salam and G. Soyez, *The anti- k_t jet clustering algorithm*, *JHEP* **04** (2008) 063,
arXiv: [0802.1189 \[hep-ph\]](#).
- [80] ATLAS Collaboration,
Jet energy measurement with the ATLAS detector in proton–proton collisions at $\sqrt{s} = 7$ TeV,
Eur. Phys. J. C **73** (2013) 2304, arXiv: [1112.6426 \[hep-ex\]](#).
- [81] ATLAS Collaboration, *Jet energy measurement and its systematic uncertainty in proton–proton collisions at $\sqrt{s} = 7$ TeV with the ATLAS detector*, *Eur. Phys. J. C* **75** (2015) 17,
arXiv: [1406.0076 \[hep-ex\]](#).
- [82] ATLAS Collaboration, *Performance of pile-up mitigation techniques for jets in pp collisions at $\sqrt{s} = 8$ TeV using the ATLAS detector*, *Eur. Phys. J. C* **76** (2016) 581,
arXiv: [1510.03823 \[hep-ex\]](#).
- [83] ATLAS Collaboration,
Jet global sequential corrections with the ATLAS detector in proton–proton collisions at $\sqrt{s} = 8$ TeV,
ATLAS-CONF-2015-002, 2015, URL: <https://cds.cern.ch/record/2001682>.

- [84] ATLAS Collaboration, *Jet Calibration and Systematic Uncertainties for Jets Reconstructed in the ATLAS Detector at $\sqrt{s} = 13$ TeV*, ATL-PHYS-PUB-2015-015, 2015, URL: <https://cds.cern.ch/record/2037613>.
- [85] ATLAS Collaboration, *Jet energy scale measurements and their systematic uncertainties in proton–proton collisions at $\sqrt{s} = 13$ TeV with the ATLAS detector*, *Phys. Rev. D* **96** (2017) 072002, arXiv: [1703.09665](https://arxiv.org/abs/1703.09665) [hep-ex].
- [86] ATLAS Collaboration, *A measurement of the calorimeter response to single hadrons and determination of the jet energy scale uncertainty using LHC Run-1 pp-collision data with the ATLAS detector*, *Eur. Phys. J. C* **77** (2017) 26, arXiv: [1607.08842](https://arxiv.org/abs/1607.08842) [hep-ex].
- [87] ATLAS Collaboration, *ATLAS b-jet identification performance and efficiency measurement with $t\bar{t}$ events in pp collisions at $\sqrt{s} = 13$ TeV*, *Eur. Phys. J. C* **79** (2019) 970, arXiv: [1907.05120](https://arxiv.org/abs/1907.05120) [hep-ex].
- [88] ATLAS Collaboration, *Optimisation and performance studies of the ATLAS b-tagging algorithms for the 2017-18 LHC run*, ATL-PHYS-PUB-2017-013, 2017, URL: <https://cds.cern.ch/record/2273281>.
- [89] CMS Collaboration, *Search for new long-lived particles at $\sqrt{s} = 13$ TeV*, *Phys. Lett. B* **780** (2018) 432, arXiv: [1711.09120](https://arxiv.org/abs/1711.09120) [hep-ex].
- [90] ATLAS Collaboration, *Measurement of the charged-particle multiplicity inside jets from $\sqrt{s} = 8$ TeV pp collisions with the ATLAS detector*, *Eur. Phys. J. C* **76** (2016) 322, arXiv: [1602.00988](https://arxiv.org/abs/1602.00988) [hep-ex].
- [91] ATLAS Collaboration, *Jet energy scale and resolution measured in proton–proton collisions at $\sqrt{s} = 13$ TeV with the ATLAS detector*, (2020), arXiv: [2007.02645](https://arxiv.org/abs/2007.02645) [hep-ex].
- [92] ATLAS Collaboration, *Transverse momentum response and reconstruction efficiency for jets from displaced decays in the ATLAS detector*, ATL-PHYS-PUB-2019-025, 2019, URL: <https://cds.cern.ch/record/2682843>.
- [93] ATLAS Collaboration, *Measurement of the Inelastic Proton–Proton Cross Section at $\sqrt{s} = 13$ TeV with the ATLAS Detector at the LHC*, *Phys. Rev. Lett.* **117** (2016) 182002, arXiv: [1606.02625](https://arxiv.org/abs/1606.02625) [hep-ex].
- [94] ATLAS Collaboration, *Early Inner Detector Tracking Performance in the 2015 Data at $\sqrt{s} = 13$ TeV*, ATL-PHYS-PUB-2015-051, 2015, URL: <https://cds.cern.ch/record/2110140>.
- [95] ATLAS Collaboration, *Luminosity determination in pp collisions at $\sqrt{s} = 13$ TeV using the ATLAS detector at the LHC*, ATLAS-CONF-2019-021, 2019, URL: <https://cds.cern.ch/record/2677054>.
- [96] G. Avoni et al., *The new LUCID-2 detector for luminosity measurement and monitoring in ATLAS*, *JINST* **13** (2018) P07017.
- [97] A. L. Read, *Presentation of search results: the CL_S technique*, *J. Phys. G* **28** (2002) 2693.
- [98] ATLAS Collaboration, *ATLAS Computing Acknowledgements*, ATL-SOFT-PUB-2021-003, URL: <https://cds.cern.ch/record/2776662>.

The ATLAS Collaboration

G. Aad¹⁰⁰, B. Abbott¹¹⁷, D.C. Abbott¹⁰¹, A. Abed Abud³⁴, K. Abeling⁵³, D.K. Abhayasinghe⁹², S.H. Abidi²⁷, H. Abramowicz¹⁴⁸, H. Abreu¹⁴⁷, Y. Abulaiti⁵, A.C. Abusleme Hoffman^{134a}, B.S. Acharya^{66a,66b,q}, B. Achkar⁵³, L. Adam⁹⁸, C. Adam Bourdarios⁴, L. Adamczyk^{82a}, L. Adamek¹⁵², J. Adelman¹¹³, A. Adiguzel^{11c,ae}, S. Adorni⁵⁴, T. Adye¹³¹, A.A. Affolder¹³³, Y. Afik¹⁴⁷, C. Agapopoulou⁶⁴, M.N. Agaras¹², J. Agarwala^{70a,70b}, A. Aggarwal¹¹¹, C. Agheorghiesei^{25c}, J.A. Aguilar-Saavedra^{127f,127a,ad}, A. Ahmad³⁴, F. Ahmadov^{36,ab}, W.S. Ahmed¹⁰², X. Ai⁴⁶, G. Aielli^{73a,73b}, S. Akatsuka⁸⁴, M. Akbiyik⁹⁸, T.P.A. Akesson⁹⁵, A.V. Akimov³⁵, K. Al Khoury³⁹, G.L. Alberghi^{21b}, J. Albert¹⁶¹, M.J. Alconada Verzini⁸⁷, S. Alderweireldt⁵⁰, M. Aleksa³⁴, I.N. Aleksandrov³⁶, C. Alexa^{25b}, T. Alexopoulos⁹, A. Alfonsi¹¹², F. Alfonsi^{21b,21a}, M. Alhroob¹¹⁷, B. Ali¹²⁹, S. Ali¹⁴⁵, M. Aliev³⁵, G. Alimonti^{68a}, C. Allaire³⁴, B.M.M. Allbrooke¹⁴³, P.P. Allport¹⁹, A. Aloisio^{69a,69b}, F. Alonso⁸⁷, C. Alpigiani¹³⁵, E. Alunno Camelia^{73a,73b}, M. Alvarez Estevez⁹⁷, M.G. Alvigi^{69a,69b}, Y. Amaral Coutinho^{79b}, A. Ambler¹⁰², L. Ambroz¹²³, C. Amelung³⁴, D. Amidei¹⁰⁴, S.P. Amor Dos Santos^{127a}, S. Amoroso⁴⁶, C.S. Amrouche⁵⁴, C. Anastopoulos¹³⁶, N. Andari¹³², T. Andeen¹⁰, J.K. Anders¹⁸, S.Y. Andrean^{45a,45b}, A. Andreazza^{68a,68b}, V. Andrei^{61a}, S. Angelidakis⁸, A. Angerami³⁹, A.V. Anisenkov³⁵, A. Annovi^{71a}, C. Antel⁵⁴, M.T. Anthony¹³⁶, E. Antipov¹¹⁸, M. Antonelli⁵¹, D.J.A. Antrim^{16a}, F. Anulli^{72a}, M. Aoki⁸⁰, J.A. Aparisi Pozo¹⁵⁹, M.A. Aparo¹⁴³, L. Aperio Bella⁴⁶, N. Aranzabal³⁴, V. Araujo Ferraz^{79a}, C. Arcangeletti⁵¹, A.T.H. Arce⁴⁹, E. Arena⁸⁹, J-F. Arguin¹⁰⁶, S. Argyropoulos⁵², J.-H. Arling⁴⁶, A.J. Armbruster³⁴, A. Armstrong¹⁵⁶, O. Arnaez¹⁵², H. Arnold³⁴, Z.P. Arrubarrena Tame¹⁰⁷, G. Artoni¹²³, H. Asada¹⁰⁹, K. Asai¹¹⁵, S. Asai¹⁵⁰, N.A. Asbah⁵⁹, E.M. Asimakopoulou¹⁵⁷, L. Asquith¹⁴³, K. Assamagan²⁷, R. Astalos^{26a}, R.J. Atkin^{31a}, M. Atkinson¹⁵⁸, N.B. Atlay¹⁷, H. Atmani^{60b}, P.A. Atlasiddha¹⁰⁴, K. Augsten¹²⁹, S. Auricchio^{69a,69b}, V.A. Austrup¹⁶⁷, G. Avolio³⁴, M.K. Ayoub^{13c}, G. Azuelos^{106,ak}, D. Babal^{26a}, H. Bachacou¹³², K. Bachas¹⁴⁹, F. Backman^{45a,45b}, A. Badea⁵⁹, P. Bagnaia^{72a,72b}, H. Bahrasemani¹³⁹, A.J. Bailey¹⁵⁹, V.R. Bailey¹⁵⁸, J.T. Baines¹³¹, C. Bakalis⁹, O.K. Baker¹⁶⁸, P.J. Bakker¹¹², E. Bakos¹⁴, D. Bakshi Gupta⁷, S. Balaji¹⁴⁴, R. Balasubramanian¹¹², E.M. Baldin³⁵, P. Balek¹³⁰, E. Ballabene^{68a,68b}, F. Balli¹³², W.K. Balunas¹²³, J. Balz⁹⁸, E. Banas⁸³, M. Bandieramonte¹²⁶, A. Bandyopadhyay¹⁷, L. Barak¹⁴⁸, E.L. Barberio¹⁰³, D. Barberis^{55b,55a}, M. Barbero¹⁰⁰, G. Barbour⁹³, K.N. Barends^{31a}, T. Barillari¹⁰⁸, M-S. Barisits³⁴, J. Barkeloo¹²⁰, T. Barklow¹⁴⁰, B.M. Barnett¹³¹, R.M. Barnett^{16a}, A. Baroncelli^{60a}, G. Barone²⁷, A.J. Barr¹²³, L. Barranco Navarro^{45a,45b}, F. Barreiro⁹⁷, J. Barreiro Guimarães da Costa^{13a}, U. Barron¹⁴⁸, S. Barsov³⁵, F. Bartels^{61a}, R. Bartoldus¹⁴⁰, G. Bartolini¹⁰⁰, A.E. Barton⁸⁸, P. Bartos^{26a}, A. Basalaev⁴⁶, A. Basan⁹⁸, I. Bashta^{74a,74b}, A. Bassalat^{64,ag}, M.J. Basso¹⁵², C.R. Basson⁹⁹, R.L. Bates⁵⁷, S. Batlamous^{33e}, J.R. Batley³⁰, B. Batool¹³⁸, M. Battaglia¹³³, M. Baucé^{72a,72b}, F. Bauer^{132,*}, P. Bauer²², H.S. Bawa²⁹, A. Bayirli^{11c}, J.B. Beacham⁴⁹, T. Beau¹²⁴, P.H. Beauchemin¹⁵⁵, F. Becherer⁵², P. Bechtel²², H.P. Beck^{18,s}, K. Becker¹⁶³, C. Becot⁴⁶, A.J. Beddall^{11a}, V.A. Bednyakov³⁶, C.P. Bee¹⁴², T.A. Beermann¹⁶⁷, M. Begalli^{79b}, M. Begel²⁷, A. Behera¹⁴², J.K. Behr⁴⁶, C. Beirao Da Cruz E Silva³⁴, J.F. Beirer^{53,34}, F. Beisiegel²², M. Belfkir⁴, G. Bella¹⁴⁸, L. Bellagamba^{21b}, A. Bellerive³², P. Bellos¹⁹, K. Beloborodov³⁵, K. Belotskiy³⁵, N.L. Belyaev³⁵, D. Bencheekroun^{33a}, Y. Benhammou¹⁴⁸, D.P. Benjamin²⁷, M. Benoit²⁷, J.R. Bensinger²⁴, S. Bentvelsen¹¹², L. Beresford³⁴, M. Beretta⁵¹, D. Berge¹⁷, E. Bergeaas Kuutmann¹⁵⁷, N. Berger⁴, B. Bergmann¹²⁹, L.J. Bergsten²⁴, J. Beringer^{16a}, S. Berlendis⁶, G. Bernardi¹²⁴, C. Bernius¹⁴⁰, F.U. Bernlochner²², T. Berry⁹², P. Berta⁴⁶, A. Berthold⁴⁸, I.A. Bertram⁸⁸, O. Bessidskaia Bylund¹⁶⁷, S. Bethke¹⁰⁸, A. Betti⁴², A.J. Bevan⁹¹, S. Bhatta¹⁴², D.S. Bhattacharya¹⁶², P. Bhattarai²⁴, V.S. Bhopatkar⁵, R. Bi¹²⁶, R.M. Bianchi¹²⁶, O. Biebel¹⁰⁷, R. Bielski³⁴, N.V. Biesuz^{71a,71b}, M. Biglietti^{74a}, T.R.V. Billoud¹²⁹, M. Bindi⁵³, A. Bingul^{11d}, C. Bini^{72a,72b}, S. Biondi^{21b,21a}, C.J. Birch-sykes⁹⁹, G.A. Bird^{19,131}, M. Birman¹⁶⁵, T. Bisanz³⁴, D. Biswas^{166,1}, A. Bitadze⁹⁹, C. Bittrich⁴⁸, K. Björke¹²², I. Bloch⁴⁶,

C. Blocker²⁴, A. Blue⁵⁷, U. Blumenschein⁹¹, J. Blumenthal⁹⁸, G.J. Bobbink¹¹², V.S. Bobrovnikov³⁵,
 D. Bogavac¹², A.G. Bogdanchikov³⁵, C. Bohm^{45a}, V. Boisvert⁹², P. Bokan⁴⁶, T. Bold^{82a}, M. Bomben¹²⁴,
 M. Bona⁹¹, M. Boonekamp¹³², C.D. Booth⁹², A.G. Borbély⁵⁷, H.M. Borecka-Bielska¹⁰⁶, L.S. Borgna⁹³,
 G. Borissov⁸⁸, D. Bortoletto¹²³, D. Boscherini^{21b}, M. Bosman¹², J.D. Bossio Sola¹⁰², K. Bouaouda^{33a},
 J. Boudreau¹²⁶, E.V. Bouhova-Thacker⁸⁸, D. Boumediene³⁸, R. Bouquet¹²⁴, A. Boveia¹¹⁶, J. Boyd³⁴,
 D. Boye²⁷, I.R. Boyko³⁶, A.J. Bozson⁹², J. Bracinik¹⁹, N. Brahimi^{60d,60c}, G. Brandt¹⁶⁷, O. Brandt³⁰,
 F. Braren⁴⁶, B. Brau¹⁰¹, J.E. Brau¹²⁰, W.D. Breaden Madden⁵⁷, K. Brendlinger⁴⁶, R. Brenner¹⁶⁵,
 L. Brenner³⁴, R. Brenner¹⁵⁷, S. Bressler¹⁶⁵, B. Brickwedde⁹⁸, D.L. Briglin¹⁹, D. Britton⁵⁷, D. Britzger¹⁰⁸,
 I. Brock²², R. Brock¹⁰⁵, G. Brooijmans³⁹, W.K. Brooks^{134e}, E. Brost²⁷, P.A. Bruckman de Renstrom⁸³,
 B. Brüers⁴⁶, D. Bruncko^{26b,*}, A. Bruni^{21b}, G. Bruni^{21b}, M. Bruschi^{21b}, N. Brusino^{72a,72b},
 L. Bryngemark¹⁴⁰, T. Buanes¹⁵, Q. Buat¹⁴², P. Buchholz¹³⁸, A.G. Buckley⁵⁷, I.A. Budagov^{36,*},
 M.K. Bugge¹²², O. Bulekov³⁵, B.A. Bullard⁵⁹, T.J. Burch¹¹³, S. Burdin⁸⁹, C.D. Burgard⁴⁶, A.M. Burger¹¹⁸,
 B. Burghgrave⁷, J.T.P. Burr⁴⁶, C.D. Burton¹⁰, J.C. Burzynski¹⁰¹, V. Büscher⁹⁸, P.J. Bussey⁵⁷,
 J.M. Butler²³, C.M. Buttar⁵⁷, J.M. Butterworth⁹³, W. Buttinger¹³¹, C.J. Buxo Vazquez¹⁰⁵,
 A.R. Buzykaev³⁵, G. Cabras^{21b}, S. Cabrera Urbán¹⁵⁹, D. Caforio⁵⁶, H. Cai¹²⁶, V.M.M. Cairo¹⁴⁰,
 O. Cakir^{3a}, N. Calace³⁴, P. Calafiura^{16a}, G. Calderini¹²⁴, P. Calfayan⁶⁵, G. Callea⁵⁷, L.P. Caloba^{79b},
 A. Caltabiano^{73a,73b}, S. Calvente Lopez⁹⁷, D. Calvet³⁸, S. Calvet³⁸, T.P. Calvet¹⁰⁰, M. Calvetti^{71a,71b},
 R. Camacho Toro¹²⁴, S. Camarda³⁴, D. Camarero Munoz⁹⁷, P. Camarri^{73a,73b}, M.T. Camerlingo^{74a,74b},
 D. Cameron¹²², C. Camincher¹⁶¹, M. Campanelli⁹³, A. Camplani⁴⁰, V. Canale^{69a,69b}, A. Canesse¹⁰²,
 M. Cano Bret⁷⁷, J. Cantero¹¹⁸, Y. Cao¹⁵⁸, M. Capua^{41b,41a}, A. Carbone^{68a,68b}, R. Cardarelli^{73a},
 F. Cardillo¹⁵⁹, T. Carli³⁴, G. Carlino^{69a}, B.T. Carlson¹²⁶, E.M. Carlson^{161,153a}, L. Carminati^{68a,68b},
 M. Carnesale^{72a,72b}, R.M.D. Carney¹⁴⁰, S. Caron¹¹¹, E. Carquin^{134e}, S. Carrá⁴⁶, G. Carratta^{21b,21a},
 J.W.S. Carter¹⁵², T.M. Carter⁵⁰, D. Casadei^{31c}, M.P. Casado^{12,i}, A.F. Casha¹⁵², E.G. Castiglia¹⁶⁸,
 F.L. Castillo^{61a}, L. Castillo Garcia¹², V. Castillo Gimenez¹⁵⁹, N.F. Castro^{127a,127e}, A. Catinaccio³⁴,
 J.R. Catmore¹²², A. Cattai³⁴, V. Cavaliere²⁷, N. Cavalli^{21b,21a}, V. Cavasinni^{71a,71b}, E. Celebi^{11b}, F. Celli¹²³,
 K. Cerny¹¹⁹, A.S. Cerqueira^{79a}, A. Cerri¹⁴³, L. Cerrito^{73a,73b}, F. Cerutti^{16a}, A. Cervelli^{21b}, S.A. Cetin^{11b},
 Z. Chadi^{33a}, D. Chakraborty¹¹³, M. Chala^{127f}, J. Chan¹⁶⁶, W.S. Chan¹¹², W.Y. Chan⁸⁹, J.D. Chapman³⁰,
 B. Chargeishvili^{146b}, D.G. Charlton¹⁹, T.P. Charman⁹¹, M. Chatterjee¹⁸, C.C. Chau³², S. Chekanov⁵,
 S.V. Chekulaev^{153a}, G.A. Chelkov^{36,a}, A. Chen¹⁰⁴, B. Chen¹⁴⁸, C. Chen^{60a}, C.H. Chen⁷⁸, H. Chen^{13c},
 H. Chen²⁷, J. Chen^{60a}, J. Chen³⁹, J. Chen²⁴, S. Chen¹²⁵, S.J. Chen^{13c}, X. Chen^{13b,aj}, Y. Chen^{60a},
 Y-H. Chen⁴⁶, C.L. Cheng¹⁶⁶, H.C. Cheng^{62a}, H.J. Cheng^{13a}, A. Cheplakov³⁶, E. Cheremushkina⁴⁶,
 R. Cherkaoui El Moursli^{33e}, E. Cheu⁶, K. Cheung⁶³, L. Chevalier¹³², V. Chiarella⁵¹, G. Chiarelli^{71a},
 G. Chiodini^{67a}, A.S. Chisholm¹⁹, A. Chitan^{25b}, I. Chiu¹⁵⁰, Y.H. Chiu¹⁶¹, M.V. Chizhov^{36,t}, K. Choi¹⁰,
 A.R. Chomont^{72a,72b}, Y. Chou¹⁰¹, E.Y.S. Chow¹¹², L.D. Christopher^{31f}, M.C. Chu^{62a}, X. Chu^{13a,13d},
 J. Chudoba¹²⁸, J.J. Chwastowski⁸³, D. Cieri¹⁰⁸, K.M. Ciesla⁸³, V. Cindro⁹⁰, I.A. Cioară^{25b}, A. Ciocio^{16a},
 F. Ciotto^{69a,69b}, Z.H. Citron^{165,m}, M. Citterio^{68a}, D.A. Ciubotaru^{25b}, B.M. Ciungu¹⁵², A. Clark⁵⁴,
 P.J. Clark⁵⁰, J.M. Clavijo Columbie⁴⁶, S.E. Clawson⁹⁹, C. Clement^{45a,45b}, L. Clissa^{21b,21a}, Y. Coadou¹⁰⁰,
 M. Cokal^{66a,66c}, A. Coccaro^{55b}, J. Cochran⁷⁸, R.F. Coelho Barrue^{127a}, R. Coelho Lopes De Sa¹⁰¹,
 S. Coelli^{68a}, H. Cohen¹⁴⁸, A.E.C. Coimbra³⁴, B. Cole³⁹, J. Collot⁵⁸, P. Conde Muñio^{127a,127h},
 S.H. Connell^{31c}, I.A. Connelly⁵⁷, E.I. Conroy¹²³, F. Conventi^{69a,al}, H.G. Cooke¹⁹, A.M. Cooper-Sarkar¹²³,
 F. Cormier¹⁶⁰, L.D. Corpe³⁴, M. Corradi^{72a,72b}, E.E. Corrigan⁹⁵, F. Corriveau^{102,aa}, M.J. Costa¹⁵⁹,
 F. Costanza⁴, D. Costanzo¹³⁶, B.M. Cote¹¹⁶, G. Cowan⁹², J.W. Cowley³⁰, J. Crane⁹⁹, K. Cranmer¹¹⁴,
 R.A. Creager¹²⁵, S. Crépe-Renaudin⁵⁸, F. Crescioli¹²⁴, M. Cristinziani¹³⁸, M. Cristoforetti^{75a,75b,c},
 V. Croft¹⁵⁵, G. Crosetti^{41b,41a}, A. Cueto⁴, T. Cuhadar Donszelmann¹⁵⁶, H. Cui^{13a,13d}, A.R. Cukierman¹⁴⁰,
 W.R. Cunningham⁵⁷, S. Czekierda⁸³, P. Czodrowski³⁴, M.M. Czurylo^{61b},
 M.J. Da Cunha Sargedas De Sousa^{60a}, J.V. Da Fonseca Pinto^{79b}, C. Da Via⁹⁹, W. Dabrowski^{82a}, T. Dado⁴⁷,
 S. Dahbi^{31f}, T. Dai¹⁰⁴, C. Dallapiccola¹⁰¹, M. Dam⁴⁰, G. D'amen²⁷, V. D'Amico^{74a,74b}, J. Damp⁹⁸,

J.R. Dandoy¹²⁵, M.F. Daneri²⁸, M. Danninger¹³⁹, V. Dao³⁴, G. Darbo^{55b}, S. Darmora⁵, A. Dattagupta¹²⁰, S. D'Auria^{68a,68b}, C. David^{153b}, T. Davidek¹³⁰, D.R. Davis⁴⁹, B. Davis-Purcell³², I. Dawson⁹¹, K. De⁷, R. De Asmundis^{69a}, M. De Beurs¹¹², S. De Castro^{21b,21a}, N. De Groot¹¹¹, P. de Jong¹¹², H. De la Torre¹⁰⁵, A. De Maria^{13c}, D. De Pedis^{72a}, A. De Salvo^{72a}, U. De Sanctis^{73a,73b}, M. De Santis^{73a,73b}, A. De Santo¹⁴³, J.B. De Vivie De Regie⁵⁸, D.V. Dedovich³⁶, J. Degens¹¹², A.M. Deiana⁴², J. Del Peso⁹⁷, Y. Delabat Diaz⁴⁶, F. Deliot¹³², C.M. Delitzsch⁶, M. Della Pietra^{69a,69b}, D. Della Volpe⁵⁴, A. Dell'Acqua³⁴, L. Dell'Asta^{68a,68b}, M. Delmastro⁴, P.A. Delsart⁵⁸, S. Demers¹⁶⁸, M. Demichev³⁶, S.P. Denisov³⁵, L. D'Eramo¹¹³, D. Derendarz⁸³, J.E. Derkaoui^{33d}, F. Derue¹²⁴, P. Dervan⁸⁹, K. Desch²², K. Dette¹⁵², C. Deutsch²², P.O. Deviveiros³⁴, F.A. Di Bello^{72a,72b}, A. Di Ciaccio^{73a,73b}, L. Di Ciaccio⁴, C. Di Donato^{69a,69b}, A. Di Girolamo³⁴, G. Di Gregorio^{71a,71b}, A. Di Luca^{75a,75b}, B. Di Micco^{74a,74b}, R. Di Nardo^{74a,74b}, C. Diaconu¹⁰⁰, F.A. Dias¹¹², T. Dias Do Vale^{127a}, M.A. Diaz^{134a,134b}, F.G. Diaz Capriles²², J. Dickinson^{16a}, M. Didenko¹⁵⁹, E.B. Diehl¹⁰⁴, J. Dietrich¹⁷, S. Díez Cornell⁴⁶, C. Díez Pardos¹³⁸, A. Dimitrievska^{16a}, W. Ding^{13b}, J. Dingfelder²², I-M. Dinu^{25b}, S.J. Dittmeier^{61b}, F. Dittus³⁴, F. Djama¹⁰⁰, T. Djobava^{146b}, J.I. Djuvslund¹⁵, M.A.B. Do Vale^{79c}, D. Dodsworth²⁴, C. Doglioni⁹⁵, J. Dolejsi¹³⁰, Z. Dolezal¹³⁰, M. Donadelli^{79d}, B. Dong^{60c}, J. Donini³⁸, A. D'Onofrio^{13c}, M. D'Onofrio⁸⁹, J. Dopke¹³¹, A. Doria^{69a}, M.T. Dova⁸⁷, A.T. Doyle⁵⁷, E. Drechsler¹³⁹, E. Dreyer¹³⁹, T. Dreyer⁵³, A.S. Drobac¹⁵⁵, D. Du^{60b}, T.A. du Pree¹¹², F. Dubinin³⁵, M. Dubovsky^{26a}, A. Dubreuil⁵⁴, E. Duchovni¹⁶⁵, G. Duckeck¹⁰⁷, O.A. Ducu^{34,25b}, D. Duda¹⁰⁸, A. Dudarev³⁴, M. D'uffizi⁹⁹, L. Duflo⁶⁴, M. Dührssen³⁴, C. Dülsen¹⁶⁷, A.E. Dumitriu^{25b}, M. Dunford^{61a}, S. Dungs⁴⁷, A. Duperrin¹⁰⁰, H. Duran Yildiz^{3a}, M. Düren⁵⁶, A. Durglishvili^{146b}, B. Dutta⁴⁶, B.L. Dwyer¹¹³, G.I. Dyckes¹²⁵, M. Dyndal^{82a}, S. Dysch⁹⁹, B.S. Dziedzic⁸³, B. Eckerova^{26a}, M.G. Eggleston⁴⁹, E. Egidio Purcino De Souza^{79b}, L.F. Ehrke⁵⁴, T. Eifert⁷, G. Eigen¹⁵, K. Einsweiler^{16a}, T. Ekelof¹⁵⁷, Y. El Ghazali^{33b}, H. El Jarrari^{33e}, A. El Moussaouy^{33a}, V. Ellajosyula¹⁵⁷, M. Ellert¹⁵⁷, F. Ellinghaus¹⁶⁷, A.A. Elliot⁹¹, N. Ellis³⁴, J. Elmsheuser²⁷, M. Elsing³⁴, D. Emeliyanov¹³¹, A. Emerman³⁹, Y. Enari¹⁵⁰, J. Erdmann⁴⁷, A. Ereditato¹⁸, P.A. Erland⁸³, M. Errenst¹⁶⁷, M. Escalier⁶⁴, C. Escobar¹⁵⁹, O. Estrada Pastor¹⁵⁹, E. Etzion¹⁴⁸, G. Evans^{127a}, H. Evans⁶⁵, M.O. Evans¹⁴³, A. Ezhilov³⁵, F. Fabbri⁵⁷, L. Fabbri^{21b,21a}, V. Fabiani¹¹¹, G. Facini¹⁶³, V. Fadeyev¹³³, R.M. Fakhrutdinov³⁵, S. Falciano^{72a}, P.J. Falke²², S. Falke³⁴, J. Faltova¹³⁰, Y. Fan^{13a}, Y. Fang^{13a}, Y. Fang^{13a,13d}, G. Fanourakis⁴⁴, M. Fanti^{68a,68b}, M. Faraj^{60c}, A. Farbin⁷, A. Farilla^{74a}, E.M. Farina^{70a,70b}, T. Farooque¹⁰⁵, S.M. Farrington⁵⁰, P. Farthouat³⁴, F. Fassi^{33e}, D. Fassouliotis⁸, M. Fauci Giannelli^{73a,73b}, W.J. Fawcett³⁰, L. Fayard⁶⁴, O.L. Fedin^{35,a}, M. Feickert¹⁵⁸, L. Feligioni¹⁰⁰, A. Fell¹³⁶, C. Feng^{60b}, M. Feng^{13b}, M.J. Fenton¹⁵⁶, A.B. Fenyuk³⁵, S.W. Ferguson⁴³, J. Ferrando⁴⁶, A. Ferrari¹⁵⁷, P. Ferrari¹¹², R. Ferrari^{70a}, D. Ferrere⁵⁴, C. Ferretti¹⁰⁴, F. Fiedler⁹⁸, A. Filipčič⁹⁰, F. Filthaut¹¹¹, M.C.N. Fiolhais^{127a,127c,b}, L. Fiorini¹⁵⁹, F. Fischer¹³⁸, W.C. Fisher¹⁰⁵, T. Fitschen¹⁹, I. Fleck¹³⁸, P. Fleischmann¹⁰⁴, T. Flick¹⁶⁷, B.M. Flierl¹⁰⁷, L. Flores¹²⁵, L.R. Flores Castillo^{62a}, F.M. Follega^{75a,75b}, N. Fomin¹⁵, J.H. Foo¹⁵², G.T. Forcolin^{75a,75b}, B.C. Forland⁶⁵, A. Formica¹³², F.A. Förster¹², A.C. Forti⁹⁹, E. Fortin¹⁰⁰, M.G. Foti¹²³, D. Fournier⁶⁴, H. Fox⁸⁸, P. Francavilla^{71a,71b}, S. Francescato^{72a,72b}, M. Franchini^{21b,21a}, S. Franchino^{61a}, D. Francis³⁴, L. Franco⁴, L. Franconi¹⁸, M. Franklin⁵⁹, G. Frattari^{72a,72b}, A.C. Freegard⁹¹, P.M. Freeman¹⁹, B. Freund¹⁰⁶, W.S. Freund^{79b}, E.M. Freundlich⁴⁷, D. Froidevaux³⁴, J.A. Frost¹²³, Y. Fu^{60a}, M. Fujimoto¹¹⁵, E. Fullana Torregrosa^{159,*}, J. Fuster¹⁵⁹, A. Gabrielli^{21b,21a}, A. Gabrielli³⁴, P. Gadow⁴⁶, G. Gagliardi^{55b,55a}, L.G. Gagnon^{16a}, G.E. Gallardo¹²³, E.J. Gallas¹²³, B.J. Gallop¹³¹, R. Gamboa Goni⁹¹, K.K. Gan¹¹⁶, S. Ganguly¹⁶⁵, J. Gao^{60a}, Y. Gao⁵⁰, Y.S. Gao^{29,o}, F.M. Garay Walls^{134a}, C. García¹⁵⁹, J.E. García Navarro¹⁵⁹, J.A. García Pascual^{13a}, M. Garcia-Sciveres^{16a}, R.W. Gardner³⁷, D. Garg⁷⁷, S. Gargiulo⁵², C.A. Garner¹⁵², V. Garonne¹²², S.J. Gasiorowski¹³⁵, P. Gaspar^{79b}, G. Gaudio^{70a}, P. Gauzzi^{72a,72b}, I.L. Gavrilenko³⁵, A. Gavrilyuk³⁵, C. Gay¹⁶⁰, G. Gaycken⁴⁶, E.N. Gazis⁹, A.A. Geanta^{25b}, C.M. Gee¹³³, C.N.P. Gee¹³¹, J. Geisen⁹⁵, M. Geisen⁹⁸, C. Gemme^{55b}, M.H. Genest⁵⁸, S. Gentile^{72a,72b}, S. George⁹², T. Geralis⁴⁴, L.O. Gerlach⁵³, P. Gessinger-Befurt⁹⁸, M. Ghasemi Bostanabad¹⁶¹, M. Ghneimat¹³⁸, A. Ghosh¹⁵⁶, A. Ghosh⁷⁷, B. Giacobbe^{21b}, S. Giagu^{72a,72b}, N. Giangiacomini¹⁵²,

P. Giannetti^{71a}, A. Giannini^{69a,69b}, S.M. Gibson⁹², M. Gignac¹³³, D.T. Gil^{82b}, B.J. Gilbert³⁹, D. Gillberg³²,
 G. Gilles¹¹², N.E.K. Gillwald⁴⁶, D.M. Gingrich^{2,ak}, M.P. Giordani^{66a,66c}, P.F. Giraud¹³²,
 G. Giugliarelli^{66a,66c}, D. Giugni^{68a}, F. Giuli^{73a,73b}, I. Gkialas^{8,j}, E.L. Gkougkousis¹², P. Gkoutoumis⁹,
 L.K. Gladilin³⁵, C. Glasman⁹⁷, G.R. Gledhill¹²⁰, M. Glisic¹²⁰, I. Gnesi^{41b,e}, M. Goblirsch-Kolb²⁴,
 D. Godin¹⁰⁶, S. Goldfarb¹⁰³, T. Golling⁵⁴, D. Golubkov³⁵, J.P. Gombas¹⁰⁵, A. Gomes^{127a,127b},
 R. Goncalves Gama⁵³, R. Gonçalo^{127a,127c}, G. Gonella¹²⁰, L. Gonella¹⁹, A. Gongadze³⁶, F. Gonnella¹⁹,
 J.L. Gonski³⁹, R.Y. González Andana^{134a}, S. González de la Hoz¹⁵⁹, S. Gonzalez Fernandez¹²,
 R. Gonzalez Lopez⁸⁹, C. Gonzalez Renteria^{16a}, R. Gonzalez Suarez¹⁵⁷, S. Gonzalez-Sevilla⁵⁴,
 G.R. Gonzalvo Rodriguez¹⁵⁹, L. Goossens³⁴, N.A. Gorasia¹⁹, P.A. Gorbounov³⁵, B. Gorini³⁴,
 E. Gorini^{67a,67b}, A. Gorišek⁹⁰, A.T. Goshaw⁴⁹, M.I. Gostkin³⁶, C.A. Gottardo¹¹¹, M. Gouighri^{33b},
 V. Goumarre⁴⁶, A.G. Goussiou¹³⁵, N. Govender^{31c}, C. Goy⁴, I. Grabowska-Bold^{82a}, K. Graham³²,
 E. Gramstad¹²², S. Grancagnolo¹⁷, M. Grandi¹⁴³, V. Gratchev^{35,*}, P.M. Gravila^{25f}, F.G. Gravili^{67a,67b},
 H.M. Gray^{16a}, C. Greife²², I.M. Gregor⁴⁶, P. Grenier¹⁴⁰, K. Grevtsov⁴⁶, C. Grieco¹², N.A. Grieser¹¹⁷,
 A.A. Grillo¹³³, K. Grimm^{29,n}, S. Grinstein^{12,w}, J.-F. Grivaz⁶⁴, S. Groh⁹⁸, E. Gross¹⁶⁵, J. Grosse-Knetter⁵³,
 Z.J. Grout⁹³, C. Grud¹⁰⁴, A. Grummer¹¹⁰, J.C. Grundy¹²³, L. Guan¹⁰⁴, W. Guan¹⁶⁶, C. Gubbels¹⁶⁰,
 J. Guenther³⁴, J.G.R. Guerrero Rojas¹⁵⁹, F. Guescini¹⁰⁸, R. Gugel⁹⁸, A. Guida⁴⁶, T. Guillemin⁴,
 S. Guindon³⁴, J. Guo^{60c}, L. Guo⁶⁴, Y. Guo¹⁰⁴, R. Gupta⁴⁶, S. Gurbuz²², G. Gustavino¹¹⁷, M. Guth⁵²,
 P. Gutierrez¹¹⁷, L.F. Gutierrez Zagazeta¹²⁵, C. Gutschow⁹³, C. Guyot¹³², C. Gwenlan¹²³, C.B. Gwilliam⁸⁹,
 E.S. Haaland¹²², A. Haas¹¹⁴, M. Habedank¹⁷, C. Haber^{16a}, H.K. Hadavand⁷, A. Hadeef⁹⁸, M. Haleem¹⁶²,
 J. Haley¹¹⁸, J.J. Hall¹³⁶, G. Halladjian¹⁰⁵, G.D. Hallelwell¹⁰⁰, L. Halser¹⁸, K. Hamano¹⁶¹, H. Hamdaoui^{33e},
 M. Hamer²², G.N. Hamity⁵⁰, K. Han^{60a}, L. Han^{13c}, L. Han^{60a}, S. Han^{16a}, Y.F. Han¹⁵², K. Hanagaki⁸⁰,
 M. Hance¹³³, M.D. Hank³⁷, R. Hankache⁹⁹, E. Hansen⁹⁵, J.B. Hansen⁴⁰, J.D. Hansen⁴⁰, M.C. Hansen²²,
 P.H. Hansen⁴⁰, K. Hara¹⁵⁴, T. Harenberg¹⁶⁷, S. Harkusha³⁵, Y.T. Harris¹²³, P.F. Harrison¹⁶³,
 N.M. Hartman¹⁴⁰, N.M. Hartmann¹⁰⁷, Y. Hasegawa¹³⁷, A. Hasib⁵⁰, S. Hassani¹³², S. Haug¹⁸,
 R. Hauser¹⁰⁵, M. Havranek¹²⁹, C.M. Hawkes¹⁹, R.J. Hawkings³⁴, S. Hayashida¹⁰⁹, D. Hayden¹⁰⁵,
 C. Hayes¹⁰⁴, R.L. Hayes¹⁶⁰, C.P. Hays¹²³, J.M. Hays⁹¹, H.S. Hayward⁸⁹, S.J. Haywood¹³¹, F. He^{60a},
 Y. He¹⁵¹, Y. He¹²⁴, M.P. Heath⁵⁰, V. Hedberg⁹⁵, A.L. Heggelund¹²², N.D. Hehir⁹¹, C. Heidegger⁵²,
 K.K. Heidegger⁵², W.D. Heidorn⁷⁸, J. Heilman³², S. Heim⁴⁶, T. Heim^{16a}, B. Heinemann^{46,ah},
 J.G. Heinlein¹²⁵, J.J. Heinrich¹²⁰, L. Heinrich³⁴, J. Hejbal¹²⁸, L. Helary⁴⁶, A. Held¹¹⁴, S. Hellesund¹²²,
 C.M. Helling¹³³, S. Hellman^{45a,45b}, C. Helsens³⁴, R.C.W. Henderson⁸⁸, L. Henkelmann³⁰,
 A.M. Henriques Correia³⁴, H. Herde¹⁴⁰, Y. Hernández Jiménez¹⁴², H. Herr⁹⁸, M.G. Herrmann¹⁰⁷,
 T. Herrmann⁴⁸, G. Herten⁵², R. Hertenberger¹⁰⁷, L. Hervas³⁴, N.P. Hessey^{153a}, H. Hibi⁸¹, S. Higashino⁸⁰,
 E. Higón-Rodríguez¹⁵⁹, K.K. Hill²⁷, K.H. Hiller⁴⁶, S.J. Hillier¹⁹, M. Hils⁴⁸, I. Hinchliffe^{16a},
 F. Hinterkeuser²², M. Hirose¹²¹, S. Hirose¹⁵⁴, D. Hirschbuehl¹⁶⁷, B. Hiti⁹⁰, O. Hladik¹²⁸, J. Hobbs¹⁴²,
 R. Hobincu^{25e}, N. Hod¹⁶⁵, M.C. Hodgkinson¹³⁶, B.H. Hodgkinson³⁰, A. Hoecker³⁴, J. Hofer⁴⁶, D. Hohn⁵²,
 T. Holm²², T.R. Holmes³⁷, M. Holzbock¹⁰⁸, L.B.A.H. Hommels³⁰, B.P. Honan⁹⁹, J. Hong^{60c},
 T.M. Hong¹²⁶, J.C. Honig⁵², A. Hönle¹⁰⁸, B.H. Hooberman¹⁵⁸, W.H. Hopkins⁵, Y. Horii¹⁰⁹, P. Horn⁴⁸,
 L.A. Horyn³⁷, S. Hou¹⁴⁵, J. Howarth⁵⁷, J. Hoya⁸⁷, M. Hrabovsky¹¹⁹, A. Hrynevich³⁵, T. Hryn'ova⁴,
 P.J. Hsu⁶³, S.-C. Hsu¹³⁵, Q. Hu³⁹, S. Hu^{60c}, Y.F. Hu^{13a,13d,am}, D.P. Huang⁹³, X. Huang^{13c}, Y. Huang^{60a},
 Y. Huang^{13a}, Z. Hubacek¹²⁹, F. Hubaut¹⁰⁰, M. Huebner²², F. Huegging²², T.B. Huffman¹²³, M. Huhtinen³⁴,
 R. Hulskens⁵⁸, N. Huseynov^{36,ab}, J. Huston¹⁰⁵, J. Huth⁵⁹, R. Hyneman¹⁴⁰, S. Hyrych^{26a}, G. Iacobucci⁵⁴,
 G. Iakovidis²⁷, I. Ibragimov¹³⁸, L. Iconomidou-Fayard⁶⁴, P. Iengo³⁴, R. Ignazzi⁴⁰, R. Iguchi¹⁵⁰,
 T. Iizawa⁵⁴, Y. Ikegami⁸⁰, A. Ilg¹⁸, N. Ilic¹⁵², H. Imam^{33a}, T. Ingebretsen Carlson^{45a,45b}, G. Introzzi^{70a,70b},
 M. Iodice^{74a}, V. Ippolito^{72a,72b}, M. Ishino¹⁵⁰, W. Islam¹¹⁸, C. Issever^{17,46}, S. Istin^{11c,an},
 J.M. Iturbe Ponce^{62a}, R. Iuppa^{75a,75b}, A. Ivina¹⁶⁵, J.M. Izen⁴³, V. Izzo^{69a}, P. Jacka¹²⁸, P. Jackson¹,
 R.M. Jacobs⁴⁶, B.P. Jaeger¹³⁹, C.S. Jagfeld¹⁰⁷, G. Jäkel¹⁶⁷, K.B. Jakobi⁹⁸, K. Jakobs⁵², T. Jakoubek¹⁶⁵,
 J. Jamieson⁵⁷, K.W. Janas^{82a}, G. Jarlskog⁹⁵, A.E. Jaspan⁸⁹, N. Javadov^{36,ab}, T. Javůrek³⁴, M. Javurkova¹⁰¹,

F. Jeanneau¹³², L. Jeanty¹²⁰, J. Jejelava^{146a,ac}, P. Jenni^{52,f}, S. Jézéquel⁴, J. Jia¹⁴², Z. Jia^{13c}, Y. Jiang^{60a}, S. Jiggins⁵², J. Jimenez Pena¹⁰⁸, S. Jin^{13c}, A. Jinaru^{25b}, O. Jinnouchi¹⁵¹, H. Jivan^{31f}, P. Johansson¹³⁶, K.A. Johns⁶, C.A. Johnson⁶⁵, E. Jones¹⁶³, R.W.L. Jones⁸⁸, T.J. Jones⁸⁹, J. Jovicevic⁵³, X. Ju^{16a}, J.J. Junggeburth³⁴, A. Juste Rozas^{12,w}, A. Kaczmarek⁸³, M. Kado^{72a,72b}, H. Kagan¹¹⁶, M. Kagan¹⁴⁰, A. Kahn³⁹, C. Kahra⁹⁸, T. Kaji¹⁶⁴, E. Kajomovitz¹⁴⁷, C.W. Kalderon²⁷, A. Kaluza⁹⁸, A. Kamenshchikov³⁵, M. Kaneda¹⁵⁰, N.J. Kang¹³³, S. Kang⁷⁸, Y. Kano¹⁰⁹, J. Kanzaki⁸⁰, D. Kar^{31f}, K. Karava¹²³, M.J. Kareem^{153b}, I. Karkanas¹⁴⁹, S.N. Karpov³⁶, Z.M. Karpova³⁶, V. Kartvelishvili⁸⁸, A.N. Karyukhin³⁵, E. Kasimi¹⁴⁹, C. Kato^{60d}, J. Katzy⁴⁶, K. Kawade¹³⁷, K. Kawagoe⁸⁶, T. Kawaguchi¹⁰⁹, T. Kawamoto¹³², G. Kawamura⁵³, E.F. Kay¹⁶¹, F.I. Kaya¹⁵⁵, S. Kazakos¹², V.F. Kazanin³⁵, Y. Ke¹⁴², J.M. Keaveney^{31a}, R. Keeler¹⁶¹, J.S. Keller³², D. Kelsey¹⁴³, J.J. Kempster¹⁹, J. Kendrick¹⁹, K.E. Kennedy³⁹, O. Kepka¹²⁸, S. Kersten¹⁶⁷, B.P. Kerševan⁹⁰, S. Ketabchi Haghghat¹⁵², M. Khandoga¹²⁴, A. Khanov¹¹⁸, A.G. Kharlamov³⁵, T. Kharlamova³⁵, E.E. Khoda¹⁶⁰, T.J. Khoo¹⁷, G. Khorauli¹⁶², J. Khubua^{146b}, S. Kido⁸¹, M. Kiehn³⁴, A. Kilgallon¹²⁰, E. Kim¹⁵¹, Y.K. Kim³⁷, N. Kimura⁹³, A. Kirchhoff⁵³, D. Kirchmeier⁴⁸, J. Kirk¹³¹, A.E. Kiryunin¹⁰⁸, T. Kishimoto¹⁵⁰, D.P. Kisliuk¹⁵², V. Kitali⁴⁶, C. Kitsaki⁹, O. Kivernyk²², T. Klapdor-Kleingrothaus⁵², M. Klassen^{61a}, C. Klein³², L. Klein¹⁶², M.H. Klein¹⁰⁴, M. Klein⁸⁹, U. Klein⁸⁹, P. Klimek³⁴, A. Klimentov²⁷, F. Klimpel³⁴, T. Klingl¹²², T. Klioutchnikova³⁴, F.F. Klitzner¹⁰⁷, P. Kluit¹¹², S. Kluth¹⁰⁸, E. Kneringer⁷⁶, T.M. Knight¹⁵², A. Knue⁵², D. Kobayashi⁸⁶, M. Kobel⁴⁸, M. Kocian¹⁴⁰, T. Kodama¹⁵⁰, P. Kodyš¹³⁰, D.M. Koeck¹⁴³, P.T. Koenig²², T. Koffas³², N.M. Köhler³⁴, M. Kolb¹³², I. Koletsou⁴, T. Komarek¹¹⁹, K. Köneke⁵², A.X.Y. Kong¹, T. Kono¹¹⁵, V. Konstantinides⁹³, N. Konstantinidis⁹³, B. Konya⁹⁵, R. Kopeliānsky⁶⁵, S. Koperny^{82a}, K. Korcyl⁸³, K. Kordas¹⁴⁹, G. Koren¹⁴⁸, A. Korn⁹³, S. Korn⁵³, I. Korolkov¹², E.V. Korolkova¹³⁶, N. Korotkova³⁵, B. Kortman¹¹², O. Kortner¹⁰⁸, S. Kortner¹⁰⁸, V.V. Kostyukhin^{136,35}, A. Kotsokchagia⁶⁴, A. Kotwal⁴⁹, A. Koulouris³⁴, A. Kourkoumeli-Charalampidi^{70a,70b}, C. Kourkoumelis⁸, E. Kourlitis⁵, R. Kowalewski¹⁶¹, W. Kozanecki¹³², A.S. Kozhin³⁵, V.A. Kramarenko³⁵, G. Kramberger⁹⁰, D. Krasnopevtsev^{60a}, M.W. Krasny¹²⁴, A. Krasznahorkay³⁴, J.A. Kremer⁹⁸, J. Kretschmar⁸⁹, K. Kreul¹⁷, P. Krieger¹⁵², F. Krieter¹⁰⁷, S. Krishnamurthy¹⁰¹, A. Krishnan^{61b}, M. Krivos¹³⁰, K. Krizka^{16a}, K. Kroeninger⁴⁷, H. Kroha¹⁰⁸, J. Kroll¹²⁸, J. Kroll¹²⁵, K.S. Krowpman¹⁰⁵, U. Kruchonak³⁶, H. Krüger²², N. Krumnack⁷⁸, M.C. Kruse⁴⁹, J.A. Krzysiak⁸³, A. Kubota¹⁵¹, O. Kuchinskaia³⁵, S. Kuday^{3b}, D. Kuechler⁴⁶, J.T. Kuechler⁴⁶, S. Kuehn³⁴, T. Kuhl⁴⁶, V. Kukhtin³⁶, Y. Kulchitsky^{35,a}, S. Kuleshov^{134c}, M. Kumar^{31f}, N. Kumari¹⁰⁰, M. Kuna⁵⁸, A. Kupco¹²⁸, T. Kupfer⁴⁷, O. Kuprash⁵², H. Kurashige⁸¹, L.L. Kurchaninov^{153a}, Y.A. Kurochkin³⁵, A. Kurova³⁵, M.G. Kurth^{13a,13d}, E.S. Kuwertz³⁴, M. Kuze¹⁵¹, A.K. Kvam¹³⁵, J. Kvita¹¹⁹, T. Kwan¹⁰², C. Lacasta¹⁵⁹, F. Lacava^{72a,72b}, H. Lacker¹⁷, D. Lacour¹²⁴, N.N. Lad⁹³, E. Ladygin³⁶, R. Lafaye⁴, B. Laforge¹²⁴, T. Lagouri^{134d}, S. Lai⁵³, I.K. Lakomic^{82a}, N. Lalloue⁵⁸, J.E. Lambert¹¹⁷, S. Lammers⁶⁵, W. Lampl⁶, C. Lampoudis¹⁴⁹, E. Lançon²⁷, U. Landgraf⁵², M.P.J. Landon⁹¹, V.S. Lang⁵², J.C. Lange⁵³, R.J. Langenberg¹⁰¹, A.J. Lankford¹⁵⁶, F. Lanni²⁷, K. Lantzsck²², A. Lanza^{70a}, A. Lapertosa^{55b,55a}, J.F. Laporte¹³², T. Lari^{68a}, F. Lasagni Manghi^{21b}, M. Lassnig³⁴, V. Latonova¹²⁸, T.S. Lau^{62a}, A. Laudrain⁹⁸, A. Laurier³², M. Lavorgna^{69a,69b}, S.D. Lawlor⁹², M. Lazzaroni^{68a,68b}, B. Le⁹⁹, B. Leban⁹⁰, A. Lebedev⁷⁸, M. LeBlanc³⁴, T. LeCompte⁵, F. Ledroit-Guillon⁵⁸, A.C.A. Lee⁹³, C.A. Lee²⁷, G.R. Lee¹⁵, L. Lee⁵⁹, S.C. Lee¹⁴⁵, S. Lee⁷⁸, L.L. Leeuw^{31c}, B. Lefebvre^{153a}, H.P. Lefebvre⁹², M. Lefebvre¹⁶¹, C. Leggett^{16a}, K. Lehmann¹³⁹, N. Lehmann¹⁸, G. Lehmann Miotto³⁴, W.A. Leight⁴⁶, A. Leisos^{149,v}, M.A.L. Leite^{79d}, C.E. Leitgeb⁴⁶, R. Leitner¹³⁰, K.J.C. Leney⁴², T. Lenz²², S. Leone^{71a}, C. Leonidopoulos⁵⁰, A. Leopold¹²⁴, C. Leroy¹⁰⁶, R. Les¹⁰⁵, C.G. Lester³⁰, M. Levchenko³⁵, J. Levêque⁴, D. Levin¹⁰⁴, L.J. Levinson¹⁶⁵, D.J. Lewis¹⁹, B. Li^{13b}, B. Li^{60b}, C. Li^{60a}, C-Q. Li^{60c,60d}, H. Li^{60a}, H. Li^{60b}, J. Li^{60c}, K. Li¹³⁵, L. Li^{60c}, M. Li^{13a,13d}, Q.Y. Li^{60a}, S. Li^{60d,60c,d}, X. Li⁴⁶, Y. Li⁴⁶, Z. Li^{60b}, Z. Li¹²³, Z. Li¹⁰², Z. Li⁸⁹, Z. Liang^{13a}, M. Liberatore⁴⁶, B. Liberti^{73a}, K. Lie^{62c}, K. Lin¹⁰⁵, R.A. Linck⁶⁵, R.E. Lindley⁶, J.H. Lindon², A. Linss⁴⁶, A.L. Lioni⁵⁴, E. Lipeles¹²⁵, A. Lipniacka¹⁵, T.M. Liss^{158,ai}, A. Lister¹⁶⁰, J.D. Little⁷, B. Liu^{13a}, B.X. Liu¹³⁹, J.B. Liu^{60a},

J.K.K. Liu³⁷, K. Liu^{60d,60c}, M. Liu^{60a}, M.Y. Liu^{60a}, P. Liu^{13a}, X. Liu^{60a}, Y. Liu⁴⁶, Y. Liu^{13c,13d}, Y.L. Liu¹⁰⁴, Y.W. Liu^{60a}, M. Livan^{70a,70b}, A. Lleres⁵⁸, J. Llorente Merino¹³⁹, S.L. Lloyd⁹¹, E.M. Lobodzinska⁴⁶, P. Loch⁶, S. Loffredo^{73a,73b}, T. Lohse¹⁷, K. Lohwasser¹³⁶, M. Lokajicek^{128,*}, J.D. Long¹⁵⁸, R.E. Long⁸⁸, I. Longarini^{72a,72b}, L. Longo³⁴, R. Longo¹⁵⁸, I. Lopez Paz¹², A. Lopez Solis⁴⁶, J. Lorenz¹⁰⁷, N. Lorenzo Martinez⁴, A.M. Lory¹⁰⁷, A. Lösle⁵², X. Lou^{45a,45b}, X. Lou^{13a,13d}, A. Lounis⁶⁴, J. Love⁵, P.A. Love⁸⁸, J.J. Lozano Bahilo¹⁵⁹, G. Lu^{13a,13d}, M. Lu^{60a}, S. Lu¹²⁵, Y.J. Lu⁶³, H.J. Lubatti¹³⁵, C. Luci^{72a,72b}, F.L. Lucio Alves^{13c}, A. Lucotte⁵⁸, F. Luehring⁶⁵, I. Luise¹⁴², L. Luminari^{72a}, B. Lund-Jensen¹⁴¹, N.A. Luongo¹²⁰, M.S. Lutz¹⁴⁸, D. Lynn²⁷, H. Lyons⁸⁹, R. Lysak¹²⁸, E. Lytken⁹⁵, F. Lyu^{13a}, V. Lyubushkin³⁶, T. Lyubushkina³⁶, H. Ma²⁷, L.L. Ma^{60b}, Y. Ma⁹³, D.M. Mac Donnell¹⁶¹, G. Maccarrone⁵¹, C.M. Macdonald¹³⁶, J.C. MacDonald¹³⁶, R. Madar³⁸, W.F. Mader⁴⁸, M. Madugoda Ralalage Don¹¹⁸, N. Madysa⁴⁸, J. Maeda⁸¹, T. Maeno²⁷, M. Maerker⁴⁸, V. Magerl⁵², J. Magro^{66a,66c}, D.J. Mahon³⁹, C. Maidantchik^{79b}, A. Maio^{127a,127b,127d}, K. Maj^{82a}, O. Majersky^{26a}, S. Majewski¹²⁰, N. Makovec⁶⁴, B. Malaescu¹²⁴, Pa. Malecki⁸³, V.P. Maleev³⁵, F. Malek⁵⁸, D. Malito^{41b,41a}, U. Mallik⁷⁷, C. Malone³⁰, S. Maltezos⁹, S. Malyukov³⁶, J. Mamuzic¹⁵⁹, G. Mancini⁵¹, J.P. Mandalia⁹¹, I. Mandić⁹⁰, L. Manhaes de Andrade Filho^{79a}, I.M. Maniatis¹⁴⁹, M. Manisha¹³², J. Manjarres Ramos⁴⁸, K.H. Mankinen⁹⁵, A. Mann¹⁰⁷, A. Manousos⁷⁶, B. Mansoulie¹³², I. Manthos¹⁴⁹, S. Manzoni¹¹², A. Marantis^{149,v}, L. Marchese¹²³, G. Marchiori¹²⁴, M. Marcisovsky¹²⁸, L. Marcoccia^{73a,73b}, C. Marcon⁹⁵, M. Marjanovic¹¹⁷, Z. Marshall^{16a}, S. Marti-Garcia¹⁵⁹, T.A. Martin¹⁶³, V.J. Martin⁵⁰, B. Martin dit Latour¹⁵, L. Martinelli^{72a,72b}, M. Martinez^{12,w}, P. Martinez Agullo¹⁵⁹, V.I. Martinez Outschoorn¹⁰¹, S. Martin-Haugh¹³¹, V.S. Martoiu^{25b}, A.C. Martyniuk⁹³, A. Marzin³⁴, S.R. Maschek¹⁰⁸, L. Masetti⁹⁸, T. Mashimo¹⁵⁰, J. Masik⁹⁹, A.L. Maslennikov³⁵, L. Massa^{21b}, P. Massarotti^{69a,69b}, P. Mastrandrea^{71a,71b}, A. Mastroberardino^{41b,41a}, T. Masubuchi¹⁵⁰, D. Matakias²⁷, T. Mathisen¹⁵⁷, A. Matic¹⁰⁷, N. Matsuzawa¹⁵⁰, J. Maurer^{25b}, B. Maček⁹⁰, D.A. Maximov³⁵, R. Mazini¹⁴⁵, I. Maznas¹⁴⁹, S.M. Mazza¹³³, C. Mc Ginn²⁷, J.P. Mc Gowan¹⁰², S.P. Mc Kee¹⁰⁴, T.G. McCarthy¹⁰⁸, W.P. McCormack^{16a}, E.F. McDonald¹⁰³, A.E. McDougall¹¹², J.A. Mcfayden¹⁴³, G. Mchedlidze^{146b}, M.A. McKay⁴², K.D. McLean¹⁶¹, S.J. McMahan¹³¹, P.C. McNamara¹⁰³, R.A. McPherson^{161,aa}, J.E. Mdhuli^{31f}, Z.A. Meadows¹⁰¹, S. Meehan³⁴, T. Megy³⁸, S. Mehlhase¹⁰⁷, A. Mehta⁸⁹, B. Meirose⁴³, D. Melini¹⁴⁷, B.R. Mellado Garcia^{31f}, F. Meloni⁴⁶, A. Melzer²², E.D. Mendes Gouveia^{127a}, A.M. Mendes Jacques Da Costa¹⁹, H.Y. Meng¹⁵², L. Meng³⁴, S. Menke¹⁰⁸, M. Mentink³⁴, E. Meoni^{41b,41a}, S.A.M. Merkt¹²⁶, C. Merlassino¹²³, P. Mermod^{54,*}, L. Merola^{69a,69b}, C. Meroni^{68a,68b}, G. Merz¹⁰⁴, O. Meshkov³⁵, J.K.R. Meshreki¹³⁸, J. Metcalfe⁵, A.S. Mete⁵, C. Meyer⁶⁵, J-P. Meyer¹³², M. Michetti¹⁷, R.P. Middleton¹³¹, L. Mijovic⁵⁰, G. Mikenberg¹⁶⁵, M. Mikestikova¹²⁸, M. Mikuž⁹⁰, H. Mildner¹³⁶, A. Milic¹⁵², C.D. Milke⁴², D.W. Miller³⁷, L.S. Miller³², A. Milov¹⁶⁵, D.A. Milstead^{45a,45b}, A.A. Minaenko³⁵, I.A. Minashvili^{146b}, L. Mince⁵⁷, A.I. Mincer¹¹⁴, B. Mindur^{82a}, M. Mineev³⁶, Y. Minegishi¹⁵⁰, Y. Mino⁸⁴, L.M. Mir¹², M. Miralles Lopez¹⁵⁹, M. Mironova¹²³, T. Mitani¹⁶⁴, V.A. Mitsou¹⁵⁹, M. Mittal^{160c}, O. Miu¹⁵², P.S. Miyagawa⁹¹, Y. Miyazaki⁸⁶, A. Mizukami⁸⁰, J.U. Mjörnmark⁹⁵, T. Mkrtchyan^{61a}, M. Mlynarikova¹¹³, T. Moe^{45a,45b}, S. Mobius⁵³, K. Mochizuki¹⁰⁶, P. Moder⁴⁶, P. Mogg¹⁰⁷, A.F. Mohammed^{13a,13d}, S. Mohapatra³⁹, G. Mokgatitswane^{31f}, B. Mondal¹³⁸, S. Mondal¹²⁹, K. Mönig⁴⁶, E. Monnier¹⁰⁰, A. Montalbano¹³⁹, J. Montejo Berlingen³⁴, M. Montella¹¹⁶, F. Monticelli⁸⁷, N. Morange⁶⁴, A.L. Moreira De Carvalho^{127a}, M. Moreno Llácer¹⁵⁹, C. Moreno Martinez¹², P. Morettini^{55b}, M. Morgenstern¹⁴⁷, S. Morgenstern¹⁶³, D. Mori¹³⁹, M. Morii⁵⁹, M. Morinaga¹⁵⁰, V. Morisbak¹²², A.K. Morley³⁴, A.P. Morris⁹³, L. Morvaj³⁴, P. Moschovakos³⁴, B. Moser¹¹², M. Mosidze^{146b}, T. Moskalets⁵², P. Moskvitina¹¹¹, J. Moss^{29,p}, E.J.W. Moyse¹⁰¹, S. Muanza¹⁰⁰, J. Mueller¹²⁶, D. Muenstermann⁸⁸, G.A. Mullier⁹⁵, J.J. Mullin¹²⁵, D.P. Mungo^{68a,68b}, J.L. Munoz Martinez¹², F.J. Munoz Sanchez⁹⁹, M. Murin⁹⁹, P. Murin^{26b}, W.J. Murray^{163,131}, A. Murrone^{68a,68b}, J.M. Muse¹¹⁷, M. Muškinja^{16a}, C. Mwewa²⁷, A.G. Myagkov^{35,a}, A.A. Myers¹²⁶, G. Myers⁶⁵, M. Myska¹²⁹, B.P. Nachman^{16a}, O. Nackenhorst⁴⁷, A. Nag⁴⁸, K. Nagai¹²³, K. Nagano⁸⁰,

J.L. Nagle²⁷, E. Nagy¹⁰⁰, A.M. Nairz³⁴, Y. Nakahama¹⁰⁹, K. Nakamura⁸⁰, H. Nanjo¹²¹, F. Napolitano^{61a},
 R. Narayan⁴², I. Naryshkin³⁵, M. Naseri³², C. Nass²², T. Naumann⁴⁶, G. Navarro^{20a},
 J. Navarro-Gonzalez¹⁵⁹, P.Y. Nechaeva³⁵, F. Nechansky⁴⁶, T.J. Neep¹⁹, A. Negri^{70a,70b}, M. Negrini^{21b},
 C. Nellist¹¹¹, C. Nelson¹⁰², K. Nelson¹⁰⁴, M.E. Nelson^{45a,45b}, S. Nemecek¹²⁸, M. Nessi^{34,h},
 M.S. Neubauer¹⁵⁸, F. Neuhaus⁹⁸, J. Neundorff⁴⁶, R. Newhouse¹⁶⁰, P.R. Newman¹⁹, C.W. Ng¹²⁶, Y.S. Ng¹⁷,
 Y.W.Y. Ng¹⁵⁶, B. Ngair^{33e}, H.D.N. Nguyen¹⁰⁰, T. Nguyen Manh¹⁰⁶, R.B. Nickerson¹²³, R. Nicolaidou¹³²,
 D.S. Nielsen⁴⁰, J. Nielsen¹³³, M. Niemeyer⁵³, N. Nikiforou¹⁰, V. Nikolaenko^{35,a}, I. Nikolic-Audit¹²⁴,
 K. Nikolopoulos¹⁹, P. Nilsson²⁷, H.R. Nindhito⁵⁴, A. Nisati^{72a}, N. Nishu², R. Nisius¹⁰⁸, T. Nitta¹⁶⁴,
 T. Nobe¹⁵⁰, D.L. Noel³⁰, Y. Noguchi⁸⁴, I. Nomidis¹²⁴, M.A. Nomura²⁷, M.B. Norfolk¹³⁶,
 R.R.B. Norisam⁹³, J. Novak⁹⁰, T. Novak⁴⁶, O. Novgorodova⁴⁸, L. Novotny¹²⁹, R. Novotny¹¹⁰, L. Nozka¹¹⁹,
 K. Ntekas¹⁵⁶, E. Nurse⁹³, F.G. Oakham^{32,ak}, J. Ocariz¹²⁴, A. Ochi⁸¹, I. Ochoa^{127a}, J.P. Ochoa-Ricoux^{134a},
 K. O'Connor²⁴, S. Oda⁸⁶, S. Odaka⁸⁰, S. Oerdek¹⁵⁷, A. Ogrodnik^{82a}, A. Oh⁹⁹, C.C. Ohm¹⁴¹, H. Oide¹⁵¹,
 R. Oishi¹⁵⁰, M.L. Ojeda¹⁵², Y. Okazaki⁸⁴, M.W. O'Keefe⁸⁹, Y. Okumura¹⁵⁰, A. Olariu^{25b},
 L.F. Oleiro Seabra^{127a}, S.A. Olivares Pino^{134d}, D. Oliveira Damazio²⁷, D. Oliveira Goncalves^{79a},
 J.L. Oliver¹, M.J.R. Olsson¹⁵⁶, A. Olszewski⁸³, J. Olszowska^{83,*}, Ö.O. Öncel²², D.C. O'Neil¹³⁹,
 A.P. O'Neill¹²³, A. Onofre^{127a,127e}, P.U.E. Onyisi¹⁰, H. Oppen¹²², R.G. Oreamuno Madriz¹¹³,
 M.J. Oreglia³⁷, G.E. Orellana⁸⁷, D. Orestano^{74a,74b}, N. Orlando¹², R.S. Orr¹⁵², V. O'Shea⁵⁷,
 R. Ospanov^{60a}, G. Otero y Garzon²⁸, H. Otono⁸⁶, P.S. Ott^{61a}, G.J. Ottino^{16a}, M. Ouchrif^{33d}, J. Ouellette²⁷,
 F. Ould-Saada¹²², A. Ouraou^{132,*}, Q. Ouyang^{13a}, M. Owen⁵⁷, R.E. Owen¹³¹, V.E. Ozcan^{11c}, N. Ozturk⁷,
 S. Ozturk^{11c}, J. Pacalt¹¹⁹, H.A. Pacey³⁰, A. Pacheco Pages¹², C. Padilla Aranda¹², S. Pagan Griso^{16a},
 G. Palacino⁶⁵, S. Palazzo⁵⁰, S. Palestini³⁴, M. Palka^{82b}, P. Palni^{82a}, D.K. Panchal¹⁰, C.E. Pandini⁵⁴,
 J.G. Panduro Vazquez⁹², P. Pani⁴⁶, G. Panizzo^{66a,66c}, L. Paolozzi⁵⁴, C. Papadatos¹⁰⁶, S. Parajuli⁴²,
 A. Paramonov⁵, C. Paraskevopoulos⁹, D. Paredes Hernandez^{62b}, S.R. Paredes Saenz¹²³, B. Parida¹⁶⁵,
 T.H. Park¹⁵², A.J. Parker²⁹, M.A. Parker³⁰, F. Parodi^{55b,55a}, E.W. Parrish¹¹³, J.A. Parsons³⁹, U. Parzefall⁵²,
 L. Pascual Dominguez¹⁴⁸, V.R. Pascuzzi^{16a}, F. Pasquali¹¹², E. Pasqualucci^{72a}, S. Passaggio^{55b}, F. Pastore⁹²,
 P. Pasuwan^{45a,45b}, J.R. Pater⁹⁹, A. Pathak¹⁶⁶, J. Patton⁸⁹, T. Pauly³⁴, J. Pearkes¹⁴⁰, M. Pedersen¹²²,
 L. Pedraza Diaz¹¹¹, R. Pedro^{127a}, T. Peiffer⁵³, S.V. Peleganchuk³⁵, O. Penc¹²⁸, C. Peng^{62b}, H. Peng^{60a},
 M. Penzin³⁵, B.S. Peralva^{79a}, M.M. Perego⁶⁴, A.P. Pereira Peixoto^{127a}, L. Pereira Sanchez^{45a,45b},
 D.V. Perepelitsa²⁷, E. Perez Codina^{153a}, M. Perganti⁹, L. Perini^{68a,68b,*}, H. Pernegger³⁴, A. Perrevoort¹¹²,
 K. Peters⁴⁶, R.F.Y. Peters⁹⁹, B.A. Petersen³⁴, T.C. Petersen⁴⁰, E. Petit¹⁰⁰, V. Petousis¹²⁹, C. Petridou¹⁴⁹,
 P. Petroff⁶⁴, F. Petrucci^{74a,74b}, M. Pettee¹⁶⁸, N.E. Pettersson³⁴, K. Petukhova¹³⁰, A. Peyaud¹³²,
 R. Pezoa^{134e}, L. Pezzotti^{70a,70b}, G. Pezzullo¹⁶⁸, T. Pham¹⁰³, P.W. Phillips¹³¹, M.W. Phipps¹⁵⁸,
 G. Piacquadio¹⁴², E. Pianori^{16a}, F. Piazza^{68a,68b}, A. Picazio¹⁰¹, R. Piegai²⁸, D. Pietreanu^{25b},
 J.E. Pilcher³⁷, A.D. Pilkington⁹⁹, M. Pinamonti^{66a,66c}, J.L. Pinfeld², C. Pitman Donaldson⁹³, D.A. Pizzi³²,
 L. Pizzimento^{73a,73b}, A. Pizzini¹¹², M.-A. Pleier²⁷, V. Plesanovs⁵², V. Pleskot¹³⁰, E. Plotnikova³⁶,
 P. Podberezko³⁵, R. Poettgen⁹⁵, R. Poggi⁵⁴, L. Poggioli¹²⁴, I. Pogrebnyak¹⁰⁵, D. Pohl²², I. Pokharel⁵³,
 G. Polesello^{70a}, A. Poley^{139,153a}, A. Policicchio^{72a,72b}, R. Polifka¹³⁰, A. Polini^{21b}, C.S. Pollard⁴⁶,
 Z.B. Pollock¹¹⁶, V. Polychronakos²⁷, D. Ponomarenko³⁵, L. Pontecorvo³⁴, S. Popa^{25a}, G.A. Popeneciu^{25d},
 L. Portales⁴, D.M. Portillo Quintero⁵⁸, S. Pospisil¹²⁹, P. Postolache^{25c}, K. Potamianos¹²³, I.N. Potrap³⁶,
 C.J. Potter³⁰, H. Potti¹, T. Poulsen⁴⁶, J. Poveda¹⁵⁹, T.D. Powell¹³⁶, G. Pownall⁴⁶, M.E. Pozo Astigarraga³⁴,
 A. Prades Ibanez¹⁵⁹, P. Pralavorio¹⁰⁰, M.M. Prapa⁴⁴, S. Prell⁷⁸, D. Price⁹⁹, M. Primavera^{67a},
 M.A. Principe Martin⁹⁷, M.L. Proffitt¹³⁵, N. Proklova³⁵, K. Prokofiev^{62c}, S. Protopopescu²⁷, J. Proudfoot⁵,
 M. Przybycien^{82a}, D. Pudza³⁵, P. Puzo⁶⁴, D. Pyatiizbyantseva³⁵, J. Qian¹⁰⁴, Y. Qin⁹⁹, A. Quadt⁵³,
 M. Queitsch-Maitland³⁴, G. Rabanal Bolanos⁵⁹, F. Ragusa^{68a,68b}, G. Rahal⁹⁶, J.A. Raine⁵⁴,
 S. Rajagopalan²⁷, K. Ran^{13a,13d}, D.F. Rassloff^{61a}, D.M. Rauch⁴⁶, S. Rave⁹⁸, B. Ravina⁵⁷, I. Ravinovich¹⁶⁵,
 M. Raymond³⁴, A.L. Read¹²², N.P. Readioff¹³⁶, D.M. Rebutti^{70a,70b}, G. Redlinger²⁷, K. Reeves⁴³,
 D. Reikher¹⁴⁸, A. Reiss⁹⁸, A. Rej¹³⁸, C. Rembser³⁴, A. Renardi⁴⁶, M. Renda^{25b}, M.B. Rendel¹⁰⁸,

A.G. Rennie⁵⁷, S. Resconi^{68a}, E.D. Resseguie^{16a}, S. Rettie⁹³, B. Reynolds¹¹⁶, E. Reynolds¹⁹,
 M. Rezaei Estabragh¹⁶⁷, O.L. Rezanova³⁵, P. Reznicek¹³⁰, E. Ricci^{75a,75b}, R. Richter¹⁰⁸, S. Richter⁴⁶,
 E. Richter-Was^{82b}, M. Ridel¹²⁴, P. Rieck¹⁰⁸, P. Riedler³⁴, O. Rifki⁴⁶, M. Rijssenbeek¹⁴², A. Rimoldi^{70a,70b},
 M. Rimoldi⁴⁶, L. Rinaldi^{21b,21a}, T.T. Rinn¹⁵⁸, M.P. Rinnagel¹⁰⁷, G. Ripellino¹⁴¹, I. Riu¹², P. Rivadeneira⁴⁶,
 J.C. Rivera Vergara¹⁶¹, F. Rizatdinova¹¹⁸, E. Rizvi⁹¹, C. Rizzi⁵⁴, B.A. Roberts¹⁶³, S.H. Robertson^{102,aa},
 M. Robin⁴⁶, D. Robinson³⁰, C.M. Robles Gajardo^{134e}, M. Robles Manzano⁹⁸, A. Robson⁵⁷,
 A. Rocchi^{73a,73b}, C. Roda^{71a,71b}, S. Rodriguez Bosca^{61a}, A. Rodriguez Rodriguez⁵²,
 A.M. Rodríguez Vera^{153b}, S. Roe³⁴, A.R. Roepe-Gier¹¹⁷, J. Roggel¹⁶⁷, O. Røhne¹²², R.A. Rojas^{134e},
 B. Roland⁵², C.P.A. Roland⁶⁵, J. Roloff²⁷, A. Romaniouk³⁵, M. Romano^{21b}, N. Rompotis⁸⁹,
 M. Ronzani¹¹⁴, L. Roos¹²⁴, S. Rosati^{72a}, G. Rosin¹⁰¹, B.J. Rosser¹²⁵, E. Rossi¹⁵², E. Rossi⁴, E. Rossi^{69a,69b},
 L.P. Rossi^{55b}, L. Rossini⁴⁶, R. Rosten¹¹⁶, M. Rotaru^{25b}, B. Rottler⁵², D. Rousseau⁶⁴, D. Rousso³⁰,
 G. Rovelli^{70a,70b}, A. Roy¹⁰, A. Rozanov¹⁰⁰, Y. Rozen¹⁴⁷, X. Ruan^{31f}, A.J. Ruby⁸⁹, T.A. Ruggeri¹,
 F. Rühr⁵², A. Ruiz-Martinez¹⁵⁹, A. Rummler³⁴, Z. Rurikova⁵², N.A. Rusakovich³⁶, H.L. Russell³⁴,
 L. Rustige³⁸, J.P. Rutherford⁶, E.M. Rüttinger¹³⁶, M. Rybar¹³⁰, E.B. Rye¹²², A. Ryzhov³⁵,
 J.A. Sabater Iglesias⁴⁶, P. Sabatini¹⁵⁹, L. Sabetta^{72a,72b}, H.F.W. Sadrozinski¹³³, F. Safai Tehrani^{72a},
 B. Safarzadeh Samani¹⁴³, M. Safdari¹⁴⁰, P. Saha¹¹³, S. Saha¹⁰², M. Sahinsoy¹⁰⁸, A. Sahu¹⁶⁷,
 M. Saimpert¹³², M. Saito¹⁵⁰, T. Saito¹⁵⁰, D. Salamani⁵⁴, G. Salamanna^{74a,74b}, A. Salnikov¹⁴⁰, J. Salt¹⁵⁹,
 A. Salvador Salas¹², D. Salvatore^{41b,41a}, F. Salvatore¹⁴³, A. Salzburger³⁴, D. Sammel⁵², D. Sampsonidis¹⁴⁹,
 D. Sampsonidou^{60d,60c}, J. Sánchez¹⁵⁹, A. Sanchez Pineda⁴, V. Sanchez Sebastian¹⁵⁹, H. Sandaker¹²²,
 C.O. Sander⁴⁶, I.G. Sanderswood⁸⁸, J.A. Sandesara¹⁰¹, M. Sandhoff¹⁶⁷, C. Sandoval^{20b}, D.P.C. Sankey¹³¹,
 M. Sannino^{55b,55a}, Y. Sano¹⁰⁹, A. Sansoni⁵¹, C. Santoni³⁸, H. Santos^{127a,127b}, S.N. Santpur^{16a},
 A. Santra¹⁶⁵, K.A. Saoucha¹³⁶, J.G. Saraiva^{127a,127d}, J. Sardain¹⁰⁰, O. Sasaki⁸⁰, K. Sato¹⁵⁴, C. Sauer^{61b},
 F. Sauerburger⁵², E. Sauvan⁴, P. Savard^{152,ak}, R. Sawada¹⁵⁰, C. Sawyer¹³¹, L. Sawyer⁹⁴,
 I. Sayago Galvan¹⁵⁹, C. Sbarra^{21b}, A. Sbrizzi^{66a,66c}, T. Scanlon⁹³, J. Schaarschmidt¹³⁵, P. Schacht¹⁰⁸,
 D. Schaefer³⁷, L. Schaefer¹²⁵, U. Schäfer⁹⁸, A.C. Schaffer⁶⁴, D. Schaile¹⁰⁷, R.D. Schamberger¹⁴²,
 E. Schanet¹⁰⁷, C. Scharf¹⁷, N. Scharmberg⁹⁹, V.A. Schegelsky³⁵, D. Scheirich¹³⁰, F. Schenck¹⁷,
 M. Schernau¹⁵⁶, C. Schiavi^{55b,55a}, L.K. Schildgen²², Z.M. Schillaci²⁴, E.J. Schioppa^{67a,67b},
 M. Schioppa^{41b,41a}, B. Schlag⁹⁸, K.E. Schleicher⁵², S. Schlenker³⁴, K. Schmieden⁹⁸, C. Schmitt⁹⁸,
 S. Schmitt⁴⁶, L. Schoeffel¹³², A. Schoening^{61b}, P.G. Scholer⁵², E. Schopf¹²³, M. Schott⁹⁸,
 J. Schovancova³⁴, S. Schramm⁵⁴, F. Schroeder¹⁶⁷, H-C. Schultz-Coulon^{61a}, M. Schumacher⁵²,
 B.A. Schumm¹³³, Ph. Schune¹³², A. Schwartzman¹⁴⁰, T.A. Schwarz¹⁰⁴, Ph. Schwemling¹³²,
 R. Schwienhorst¹⁰⁵, A. Sciandra¹³³, G. Sciolla²⁴, F. Scuri^{71a}, F. Scutti¹⁰³, C.D. Sebastiani⁸⁹,
 K. Sedlaczek⁴⁷, P. Seema¹⁷, S.C. Seidel¹¹⁰, A. Seiden¹³³, B.D. Seidlitz²⁷, T. Seiss³⁷, C. Seitz⁴⁶,
 J.M. Seixas^{79b}, G. Sekhniaidze^{69a}, S.J. Sekula⁴², L. Selem⁴, N. Semprini-Cesari^{21b,21a}, S. Sen⁴⁹,
 C. Serfon²⁷, L. Serin⁶⁴, L. Serkin^{66a,66b}, M. Sessa^{60a}, H. Severini¹¹⁷, S. Sevova¹⁴⁰, F. Sforza^{55b,55a},
 A. Sfyrila⁵⁴, E. Shabalina⁵³, R. Shaheen¹⁴¹, J.D. Shahinian¹²⁵, N.W. Shaikh^{45a,45b}, D. Shaked Renous¹⁶⁵,
 L.Y. Shan^{13a}, M. Shapiro^{16a}, A. Sharma³⁴, A.S. Sharma¹, S. Sharma⁴⁶, P.B. Shatalov³⁵, K. Shaw¹⁴³,
 S.M. Shaw⁹⁹, P. Sherwood⁹³, L. Shi⁹³, C.O. Shimmin¹⁶⁸, Y. Shimogama¹⁶⁴, J.D. Shinner⁹²,
 I.P.J. Shipsey¹²³, S. Shirabe⁵⁴, M. Shiyakova^{36,y}, J. Shlomi¹⁶⁵, M.J. Shochet³⁷, J. Shojai¹⁰³,
 D.R. Shope¹⁴¹, S. Shrestha¹¹⁶, E.M. Shrif^{31f}, M.J. Shroff¹⁶¹, E. Shulga¹⁶⁵, P. Sicho¹²⁸, A.M. Sickles¹⁵⁸,
 E. Sideras Haddad^{31f}, O. Sidiropoulou³⁴, A. Sidoti^{21b}, F. Siegert⁴⁸, Dj. Sijacki¹⁴, M.V. Silva Oliveira³⁴,
 S.B. Silverstein^{45a}, S. Simion⁶⁴, R. Simoniello³⁴, S. Simsek^{11b}, P. Sinervo¹⁵², V. Sinetckii³⁵, S. Singh¹³⁹,
 S. Sinha⁴⁶, S. Sinha^{31f}, M. Sioli^{21b,21a}, I. Siral¹²⁰, S.Yu. Sivoklov^{35,*}, J. Sjölin^{45a,45b}, A. Skaf⁵³,
 E. Skorda⁹⁵, P. Skubic¹¹⁷, M. Slawinska⁸³, K. Sliwa¹⁵⁵, V. Smakhtin¹⁶⁵, B.H. Smart¹³¹, J. Smiesko¹³⁰,
 S.Yu. Smirnov³⁵, Y. Smirnov³⁵, L.N. Smirnova^{35,a}, O. Smirnova⁹⁵, E.A. Smith³⁷, H.A. Smith¹²³,
 M. Smizanska⁸⁸, K. Smolek¹²⁹, A. Smykiewicz⁸³, A.A. Snesarev³⁵, H.L. Snoek¹¹², S. Snyder²⁷,
 R. Sobie^{161,aa}, A. Soffer¹⁴⁸, F. Sohns⁵³, C.A. Solans Sanchez³⁴, E.Yu. Soldatov³⁵, U. Soldevila¹⁵⁹,

A.A. Solodkov³⁵, S. Solomon⁵², A. Soloshenko³⁶, O.V. Solovyanov³⁵, V. Solovyev³⁵, P. Sommer¹³⁶,
 H. Son¹⁵⁵, A. Sonay¹², W.Y. Song^{153b}, A. Sopczak¹²⁹, A.L. Sopio⁹³, F. Sopkova^{26b}, S. Sottocornola^{70a,70b},
 R. Soualah^{66a,66c}, Z. Soumami^{33e}, D. South⁴⁶, S. Spagnolo^{67a,67b}, M. Spalla¹⁰⁸, M. Spangenberg¹⁶³,
 F. Spanò⁹², D. Sperlich⁵², T.M. Spieker^{61a}, G. Spigo³⁴, M. Spina¹⁴³, D.P. Spiteri⁵⁷, M. Spousta¹³⁰,
 A. Stabile^{68a,68b}, R. Stamen^{61a}, M. Stamenkovic¹¹², A. Stampekis¹⁹, M. Standke²², E. Stanecka⁸³,
 B. Stanislaus³⁴, M.M. Stanitzki⁴⁶, M. Stankaityte¹²³, B. Stapf⁴⁶, E.A. Starchenko³⁵, G.H. Stark¹³³,
 J. Stark^{100,af}, D.M. Starko^{153b}, P. Staroba¹²⁸, P. Starovoitov^{61a}, S. Stärz¹⁰², R. Staszewski⁸³,
 G. Stavropoulos⁴⁴, P. Steinberg²⁷, A.L. Steinhebel¹²⁰, B. Stelzer^{139,153a}, H.J. Stelzer¹²⁶,
 O. Stelzer-Chilton^{153a}, H. Stenzel⁵⁶, T.J. Stevenson¹⁴³, G.A. Stewart³⁴, M.C. Stockton³⁴, G. Stoicea^{25b},
 M. Stolarski^{127a}, S. Stonjek¹⁰⁸, A. Straessner⁴⁸, J. Strandberg¹⁴¹, S. Strandberg^{45a,45b}, M. Strauss¹¹⁷,
 T. Strebler¹⁰⁰, P. Strizenec^{26b}, R. Ströhmer¹⁶², D.M. Strom¹²⁰, L.R. Strom⁴⁶, R. Stroynowski⁴²,
 A. Strubig^{45a,45b}, S.A. Stucci²⁷, B. Stugu¹⁵, J. Stupak¹¹⁷, N.A. Styles⁴⁶, D. Su¹⁴⁰, S. Su^{60a}, W. Su^{60d,135,60c},
 X. Su^{60a}, N.B. Suarez¹²⁶, K. Sugizaki¹⁵⁰, V.V. Sulin³⁵, M.J. Sullivan⁸⁹, D.M.S. Sultan⁵⁴, S. Sultansoy^{3c},
 T. Sumida⁸⁴, S. Sun¹⁰⁴, S. Sun¹⁶⁶, X. Sun⁹⁹, O. Sunneborn Gudnadottir¹⁵⁷, C.J.E. Suster¹⁴⁴,
 M.R. Sutton¹⁴³, M. Svatos¹²⁸, M. Swiatlowski^{153a}, T. Swirski¹⁶², I. Sykora^{26a}, M. Sykora¹³⁰, T. Sykora¹³⁰,
 D. Ta⁹⁸, K. Tackmann^{46,x}, A. Taffard¹⁵⁶, R. Tafirout^{153a}, E. Tagiev³⁵, R.H.M. Taibah¹²⁴, R. Takashima⁸⁵,
 K. Takeda⁸¹, T. Takeshita¹³⁷, E.P. Takeva⁵⁰, Y. Takubo⁸⁰, M. Talby¹⁰⁰, A.A. Talyshev³⁵, K.C. Tam^{62b},
 N.M. Tamir¹⁴⁸, A. Tanaka¹⁵⁰, J. Tanaka¹⁵⁰, R. Tanaka⁶⁴, Z. Tao¹⁶⁰, S. Tapia Araya⁷⁸, S. Tapprogge⁹⁸,
 A. Tarek Abouelfadl Mohamed¹⁰⁵, S. Tarem¹⁴⁷, K. Tariq^{60b}, G. Tarna^{25b,g}, G.F. Tartarelli^{68a}, P. Tas¹³⁰,
 M. Tasevsky¹²⁸, E. Tassi^{41b,41a}, G. Tateno¹⁵⁰, Y. Tayalati^{33e}, G.N. Taylor¹⁰³, W. Taylor^{153b}, H. Teagle⁸⁹,
 A.S. Tee¹⁶⁶, R. Teixeira De Lima¹⁴⁰, P. Teixeira-Dias⁹², H. Ten Kate³⁴, J.J. Teoh¹¹², K. Terashi¹⁵⁰,
 J. Terron⁹⁷, S. Terzo¹², M. Testa⁵¹, R.J. Teuscher^{152,aa}, N. Themistokleous⁵⁰, T. Thevenaux-Pelzer¹⁷,
 O. Thielmann¹⁶⁷, D.W. Thomas⁹², J.P. Thomas¹⁹, E.A. Thompson⁴⁶, P.D. Thompson¹⁹, E. Thomson¹²⁵,
 E.J. Thorpe⁹¹, Y. Tian⁵³, V. Tikhomirov^{35,a}, Yu.A. Tikhonov³⁵, S. Timoshenko³⁵, P. Tipton¹⁶⁸,
 S. Tisserant¹⁰⁰, S.H. Tlou^{31f}, A. Tmourji³⁸, K. Todome^{21b,21a}, S. Todorova-Nova¹³⁰, S. Todt⁴⁸,
 M. Togawa⁸⁰, J. Tojo⁸⁶, S. Tokár^{26a}, K. Tokushuku⁸⁰, E. Tolley¹¹⁶, R. Tombs³⁰, M. Tomoto^{80,109},
 L. Tompkins^{140,r}, P. Tornambe¹⁰¹, E. Torrence¹²⁰, H. Torres⁴⁸, E. Torró Pastor¹⁵⁹, M. Toscani²⁸,
 C. Toscirri³⁷, J. Toth^{100,z}, D.R. Tovey¹³⁶, A. Traet¹⁵, C.J. Treado¹¹⁴, T. Trefzger¹⁶², A. Tricoli²⁷,
 I.M. Trigger^{153a}, S. Trincaz-Duvoid¹²⁴, D.A. Trischuk¹⁶⁰, B. Trocmé⁵⁸, A. Trofymov⁶⁴, C. Troncon^{68a},
 F. Trovato¹⁴³, L. Truong^{31c}, M. Trzebinski⁸³, A. Trzupek⁸³, F. Tsai¹⁴², A. Tsiamis¹⁴⁹, P.V. Tsiarehshka^{35,a},
 A. Tsirigotis^{149,v}, V. Tsiskaridze¹⁴², E.G. Tskhadadze^{146a}, M. Tsopoulou¹⁴⁹, I.I. Tsukerman³⁵, V. Tsulaia^{16a},
 S. Tsuno⁸⁰, O. Tsur¹⁴⁷, D. Tsybychev¹⁴², Y. Tu^{62b}, A. Tudorache^{25b}, V. Tudorache^{25b}, A.N. Tuna³⁴,
 S. Turchikhin³⁶, D. Turgeman¹⁶⁵, I. Turk Cakir^{3b,u}, R.J. Turner¹⁹, R. Turra^{68a}, P.M. Tuts³⁹, S. Tzamarias¹⁴⁹,
 P. Tzani⁹, E. Tzovara⁹⁸, K. Uchida¹⁵⁰, F. Ukegawa¹⁵⁴, G. Unal³⁴, M. Unal¹⁰, A. Undrus²⁷, G. Unel¹⁵⁶,
 F.C. Ungaro¹⁰³, K. Uno¹⁵⁰, J. Urban^{26b}, P. Urquijo¹⁰³, G. Usai⁷, R. Ushioda¹⁵¹, M. Usman¹⁰⁶, Z. Uysal^{11d},
 V. Vacek¹²⁹, B. Vachon¹⁰², K.O.H. Vadla¹²², T. Vafeiadis³⁴, C. Valderanis¹⁰⁷, E. Valdes Santurio^{45a,45b},
 M. Valente^{153a}, S. Valentinetti^{21b,21a}, A. Valero¹⁵⁹, L. Valéry⁴⁶, R.A. Vallance¹⁹, A. Vallier^{100,af},
 J.A. Valls Ferrer¹⁵⁹, T.R. Van Daalen¹², P. Van Gemmeren⁵, S. Van Stroud⁹³, I. Van Vulpen¹¹²,
 M. Vanadia^{73a,73b}, W. Vandelli³⁴, M. Vandenbroucke¹³², E.R. Vandewall¹¹⁸, D. Vannicola^{72a,72b},
 L. Vannoli^{55b,55a}, R. Vari^{72a}, E.W. Varnes⁶, C. Varni^{55b,55a}, T. Varol¹⁴⁵, D. Varouchas⁶⁴, K.E. Varvell¹⁴⁴,
 M.E. Vasile^{25b}, L. Vaslin³⁸, G.A. Vasquez¹⁶¹, F. Vazeille³⁸, D. Vazquez Furelos¹², T. Vazquez Schroeder³⁴,
 J. Veatch⁵³, V. Vecchio⁹⁹, M.J. Veen¹¹², I. Velisek¹²³, L.M. Veloce¹⁵², F. Veloso^{127a,127c}, S. Veneziano^{72a},
 A. Ventura^{67a,67b}, A. Verbytskyi¹⁰⁸, M. Verducci^{71a,71b}, C. Vergis²², M. Verissimo De Araujo^{79b},
 W. Verkerke¹¹², A.T. Vermeulen¹¹², J.C. Vermeulen¹¹², C. Vernieri¹⁴⁰, P.J. Verschuuren⁹²,
 M.L. Vesterbacka¹¹⁴, M.C. Vetterli^{139,ak}, N. Viaux Maira^{134e}, T. Vickey¹³⁶, O.E. Vickey Boeriu¹³⁶,
 G.H.A. Viehhauser¹²³, L. Vigani^{61b}, M. Villa^{21b,21a}, M. Villaplana Perez¹⁵⁹, E.M. Villhauer⁵⁰,
 E. Vilucchi⁵¹, M.G. Vincter³², G.S. Virdee¹⁹, A. Vishwakarma⁵⁰, C. Vittori^{21b,21a}, I. Vivarelli¹⁴³,

V. Vladimirov¹⁶³, E. Voevodina¹⁰⁸, M. Vogel¹⁶⁷, P. Vokac¹²⁹, J. Von Ahnen⁴⁶, S.E. von Buddenbrock^{31f}, E. Von Toerne²², V. Vorobel¹³⁰, K. Vorobev³⁵, M. Vos¹⁵⁹, J.H. Vosseveld⁸⁹, M. Vozak⁹⁹, L. Vozdecky⁹¹, N. Vranjes¹⁴, M. Vranjes Milosavljevic¹⁴, V. Vrba^{129,*}, M. Vreeswijk¹¹², R. Vuillermet³⁴, I. Vukotic³⁷, S. Wada¹⁵⁴, C. Wagner¹⁰¹, P. Wagner²², W. Wagner¹⁶⁷, S. Wahdan¹⁶⁷, H. Wahlberg⁸⁷, R. Wakasa¹⁵⁴, M. Wakida¹⁰⁹, V.M. Walbrecht¹⁰⁸, J. Walder¹³¹, R. Walker¹⁰⁷, S.D. Walker⁹², W. Walkowiak¹³⁸, A.M. Wang⁵⁹, A.Z. Wang¹⁶⁶, C. Wang^{60a}, C. Wang^{60c}, H. Wang^{16a}, J. Wang^{62a}, P. Wang⁴², R.-J. Wang⁹⁸, R. Wang⁵⁹, R. Wang¹¹³, S.M. Wang¹⁴⁵, S. Wang^{60b}, T. Wang^{60a}, W.T. Wang^{60a}, W.X. Wang^{60a}, X. Wang¹⁵⁸, Y. Wang^{60a}, Z. Wang¹⁰⁴, A. Warburton¹⁰², C.P. Ward³⁰, R.J. Ward¹⁹, N. Warrack⁵⁷, A.T. Watson¹⁹, M.F. Watson¹⁹, G. Watts¹³⁵, B.M. Waugh⁹³, A.F. Webb¹⁰, C. Weber²⁷, M.S. Weber¹⁸, S.A. Weber³², S.M. Weber^{61a}, C. Wei^{60a}, Y. Wei¹²³, A.R. Weidberg¹²³, J. Weingarten⁴⁷, M. Weirich⁹⁸, C. Weiser⁵², T. Wenaus²⁷, B. Wendland⁴⁷, T. Wengler³⁴, S. Wenig³⁴, N. Wermes²², M. Wessels^{61a}, K. Whalen¹²⁰, A.M. Wharton⁸⁸, A.S. White⁵⁹, A. White⁷, M.J. White¹, D. Whiteson¹⁵⁶, W. Wiedenmann¹⁶⁶, C. Wiel⁴⁸, M. Wielers¹³¹, N. Wieseotte⁹⁸, C. Wiglesworth⁴⁰, L.A.M. Wiik-Fuchs⁵², D.J. Wilbern¹¹⁷, H.G. Wilkens³⁴, L.J. Wilkins⁹², D.M. Williams³⁹, H.H. Williams¹²⁵, S. Williams³⁰, S. Willocq¹⁰¹, P.J. Windischhofer¹²³, I. Wingerter-Seez⁴, F. Winklmeier¹²⁰, B.T. Winter⁵², M. Wittgen¹⁴⁰, M. Wobisch⁹⁴, A. Wolf⁹⁸, R. Wölker¹²³, J. Wollrath¹⁵⁶, M.W. Wolter⁸³, H. Wolters^{127a,127c}, V.W.S. Wong¹⁶⁰, A.F. Wongel⁴⁶, S.D. Worm⁴⁶, B.K. Wosiek⁸³, K.W. Woźniak⁸³, K. Wraight⁵⁷, J. Wu^{13a,13d}, S.L. Wu¹⁶⁶, X. Wu⁵⁴, Y. Wu^{60a}, Z. Wu^{132,60a}, J. Wuerzinger¹²³, T.R. Wyatt⁹⁹, B.M. Wynne⁵⁰, S. Xella⁴⁰, J. Xiang^{62c}, X. Xiao¹⁰⁴, X. Xie^{60a}, I. Xirotidis¹⁴³, D. Xu^{13a}, H. Xu^{60a}, H. Xu^{60a}, L. Xu^{60a}, R. Xu¹²⁵, T. Xu^{60a}, W. Xu¹⁰⁴, Y. Xu^{13b}, Z. Xu^{60b}, Z. Xu¹⁴⁰, B. Yabsley¹⁴⁴, S. Yacoob^{31a}, N. Yamaguchi⁸⁶, Y. Yamaguchi¹⁵¹, M. Yamatani¹⁵⁰, H. Yamauchi¹⁵⁴, T. Yamazaki^{16a}, Y. Yamazaki⁸¹, J. Yan^{60c}, Z. Yan²³, H.J. Yang^{60c,60d}, H.T. Yang^{16a}, S. Yang^{60a}, T. Yang^{62c}, X. Yang^{60a}, X. Yang^{13a}, Y. Yang¹⁵⁰, Z. Yang^{60a,104}, W.-M. Yao^{16a}, Y.C. Yap⁴⁶, H. Ye^{13c}, J. Ye⁴², S. Ye²⁷, I. Yeletsikh³⁶, M.R. Yexley⁸⁸, P. Yin³⁹, K. Yorita¹⁶⁴, K. Yoshihara⁷⁸, C.J.S. Young³⁴, C. Young¹⁴⁰, R. Yuan^{60b,k}, X. Yue^{61a}, M. Zaazoua^{33e}, B. Zabinski⁸³, G. Zacharis⁹, E. Zaffaroni⁵⁴, T. Zakareishvili^{146b}, N. Zakharchuk³², S. Zambito³⁴, D. Zanzi⁵², S.V. Zeißner⁴⁷, C. Zeitnitz¹⁶⁷, G. Zemaityte¹²³, J.C. Zeng¹⁵⁸, O. Zenin³⁵, T. Ženiš^{26a}, S. Zenz⁹¹, S. Zerradi^{33a}, D. Zerwas⁶⁴, M. Zgubič¹²³, B. Zhang^{13c}, D.F. Zhang^{13b}, G. Zhang^{13b}, J. Zhang⁵, K. Zhang^{13a,13d}, L. Zhang^{13c}, M. Zhang¹⁵⁸, R. Zhang¹⁶⁶, S. Zhang¹⁰⁴, X. Zhang^{60c}, X. Zhang^{60b}, Z. Zhang⁶⁴, P. Zhao⁴⁹, Y. Zhao¹³³, Z. Zhao^{60a}, A. Zhemchugov³⁶, Z. Zheng¹⁰⁴, D. Zhong¹⁵⁸, B. Zhou¹⁰⁴, C. Zhou¹⁶⁶, H. Zhou⁶, N. Zhou^{60c}, Y. Zhou⁶, C.G. Zhu^{60b}, C. Zhu^{13a,13d}, H.L. Zhu^{60a}, H. Zhu^{13a}, J. Zhu¹⁰⁴, Y. Zhu^{60a}, X. Zhuang^{13a}, K. Zhukov³⁵, V. Zhulanov³⁵, D. Zieminska⁶⁵, N.I. Zimine³⁶, S. Zimmermann^{52,*}, M. Ziolkowski¹³⁸, L. Živković¹⁴, A. Zoccoli^{21b,21a}, K. Zoch⁵⁴, T.G. Zorbas¹³⁶, O. Zormpa⁴⁴, W. Zou³⁹, L. Zwalinski³⁴.

¹Department of Physics, University of Adelaide, Adelaide; Australia.

²Department of Physics, University of Alberta, Edmonton AB; Canada.

³(^a)Department of Physics, Ankara University, Ankara; (^b)Istanbul Aydin University, Application and Research Center for Advanced Studies, Istanbul; (^c)Division of Physics, TOBB University of Economics and Technology, Ankara; Türkiye.

⁴LAPP, Université Savoie Mont Blanc, CNRS/IN2P3, Annecy; France.

⁵High Energy Physics Division, Argonne National Laboratory, Argonne IL; United States of America.

⁶Department of Physics, University of Arizona, Tucson AZ; United States of America.

⁷Department of Physics, University of Texas at Arlington, Arlington TX; United States of America.

⁸Physics Department, National and Kapodistrian University of Athens, Athens; Greece.

⁹Physics Department, National Technical University of Athens, Zografou; Greece.

¹⁰Department of Physics, University of Texas at Austin, Austin TX; United States of America.

¹¹(^a)Bahcesehir University, Faculty of Engineering and Natural Sciences, Istanbul; (^b)Istanbul Bilgi

University, Faculty of Engineering and Natural Sciences, Istanbul;^(c)Department of Physics, Bogazici University, Istanbul;^(d)Department of Physics Engineering, Gaziantep University, Gaziantep; Türkiye.

¹²Institut de Física d'Altes Energies (IFAE), Barcelona Institute of Science and Technology, Barcelona; Spain.

¹³(^a)Institute of High Energy Physics, Chinese Academy of Sciences, Beijing;^(b)Physics Department, Tsinghua University, Beijing;^(c)Department of Physics, Nanjing University, Nanjing;^(d)University of Chinese Academy of Science (UCAS), Beijing; China.

¹⁴Institute of Physics, University of Belgrade, Belgrade; Serbia.

¹⁵Department for Physics and Technology, University of Bergen, Bergen; Norway.

¹⁶(^a)Physics Division, Lawrence Berkeley National Laboratory, Berkeley CA;^(b)University of California, Berkeley CA; United States of America.

¹⁷Institut für Physik, Humboldt Universität zu Berlin, Berlin; Germany.

¹⁸Albert Einstein Center for Fundamental Physics and Laboratory for High Energy Physics, University of Bern, Bern; Switzerland.

¹⁹School of Physics and Astronomy, University of Birmingham, Birmingham; United Kingdom.

²⁰(^a)Facultad de Ciencias y Centro de Investigaciones, Universidad Antonio Nariño,

Bogotá;^(b)Departamento de Física, Universidad Nacional de Colombia, Bogotá; Colombia.

²¹(^a)Dipartimento di Fisica e Astronomia A. Righi, Università di Bologna, Bologna;^(b)INFN Sezione di Bologna; Italy.

²²Physikalisches Institut, Universität Bonn, Bonn; Germany.

²³Department of Physics, Boston University, Boston MA; United States of America.

²⁴Department of Physics, Brandeis University, Waltham MA; United States of America.

²⁵(^a)Transilvania University of Brasov, Brasov;^(b)Horia Hulubei National Institute of Physics and Nuclear Engineering, Bucharest;^(c)Department of Physics, Alexandru Ioan Cuza University of Iasi, Iasi;^(d)National Institute for Research and Development of Isotopic and Molecular Technologies, Physics Department, Cluj-Napoca;^(e)University Politehnica Bucharest, Bucharest;^(f)West University in Timisoara, Timisoara; Romania.

²⁶(^a)Faculty of Mathematics, Physics and Informatics, Comenius University, Bratislava;^(b)Department of Subnuclear Physics, Institute of Experimental Physics of the Slovak Academy of Sciences, Kosice; Slovak Republic.

²⁷Physics Department, Brookhaven National Laboratory, Upton NY; United States of America.

²⁸Universidad de Buenos Aires, Facultad de Ciencias Exactas y Naturales, Departamento de Física, y CONICET, Instituto de Física de Buenos Aires (IFIBA), Buenos Aires; Argentina.

²⁹California State University, CA; United States of America.

³⁰Cavendish Laboratory, University of Cambridge, Cambridge; United Kingdom.

³¹(^a)Department of Physics, University of Cape Town, Cape Town;^(b)iThemba Labs, Western

Cape;^(c)Department of Mechanical Engineering Science, University of Johannesburg,

Johannesburg;^(d)National Institute of Physics, University of the Philippines Diliman

(Philippines);^(e)University of South Africa, Department of Physics, Pretoria;^(f)School of Physics, University of the Witwatersrand, Johannesburg; South Africa.

³²Department of Physics, Carleton University, Ottawa ON; Canada.

³³(^a)Faculté des Sciences Ain Chock, Réseau Universitaire de Physique des Hautes Energies - Université Hassan II, Casablanca;^(b)Faculté des Sciences, Université Ibn-Tofail, Kénitra;^(c)Faculté des Sciences Semlalia, Université Cadi Ayyad, LPHEA-Marrakech;^(d)LPMR, Faculté des Sciences, Université Mohamed Premier, Oujda;^(e)Faculté des sciences, Université Mohammed V, Rabat; Morocco.

³⁴CERN, Geneva; Switzerland.

³⁵Affiliated with an institute covered by a cooperation agreement with CERN.

- ³⁶Affiliated with an international laboratory covered by a cooperation agreement with CERN.
- ³⁷Enrico Fermi Institute, University of Chicago, Chicago IL; United States of America.
- ³⁸LPC, Université Clermont Auvergne, CNRS/IN2P3, Clermont-Ferrand; France.
- ³⁹Nevis Laboratory, Columbia University, Irvington NY; United States of America.
- ⁴⁰Niels Bohr Institute, University of Copenhagen, Copenhagen; Denmark.
- ⁴¹(^a)Dipartimento di Fisica, Università della Calabria, Rende; (^b)INFN Gruppo Collegato di Cosenza, Laboratori Nazionali di Frascati; Italy.
- ⁴²Physics Department, Southern Methodist University, Dallas TX; United States of America.
- ⁴³Physics Department, University of Texas at Dallas, Richardson TX; United States of America.
- ⁴⁴National Centre for Scientific Research "Demokritos", Agia Paraskevi; Greece.
- ⁴⁵(^a)Department of Physics, Stockholm University; (^b)Oskar Klein Centre, Stockholm; Sweden.
- ⁴⁶Deutsches Elektronen-Synchrotron DESY, Hamburg and Zeuthen; Germany.
- ⁴⁷Fakultät Physik, Technische Universität Dortmund, Dortmund; Germany.
- ⁴⁸Institut für Kern- und Teilchenphysik, Technische Universität Dresden, Dresden; Germany.
- ⁴⁹Department of Physics, Duke University, Durham NC; United States of America.
- ⁵⁰SUPA - School of Physics and Astronomy, University of Edinburgh, Edinburgh; United Kingdom.
- ⁵¹INFN e Laboratori Nazionali di Frascati, Frascati; Italy.
- ⁵²Physikalisches Institut, Albert-Ludwigs-Universität Freiburg, Freiburg; Germany.
- ⁵³II. Physikalisches Institut, Georg-August-Universität Göttingen, Göttingen; Germany.
- ⁵⁴Département de Physique Nucléaire et Corpusculaire, Université de Genève, Genève; Switzerland.
- ⁵⁵(^a)Dipartimento di Fisica, Università di Genova, Genova; (^b)INFN Sezione di Genova; Italy.
- ⁵⁶II. Physikalisches Institut, Justus-Liebig-Universität Giessen, Giessen; Germany.
- ⁵⁷SUPA - School of Physics and Astronomy, University of Glasgow, Glasgow; United Kingdom.
- ⁵⁸LPSC, Université Grenoble Alpes, CNRS/IN2P3, Grenoble INP, Grenoble; France.
- ⁵⁹Laboratory for Particle Physics and Cosmology, Harvard University, Cambridge MA; United States of America.
- ⁶⁰(^a)Department of Modern Physics and State Key Laboratory of Particle Detection and Electronics, University of Science and Technology of China, Hefei; (^b)Institute of Frontier and Interdisciplinary Science and Key Laboratory of Particle Physics and Particle Irradiation (MOE), Shandong University, Qingdao; (^c)School of Physics and Astronomy, Shanghai Jiao Tong University, Key Laboratory for Particle Astrophysics and Cosmology (MOE), SKLPPC, Shanghai; (^d)Tsung-Dao Lee Institute, Shanghai; China.
- ⁶¹(^a)Kirchhoff-Institut für Physik, Ruprecht-Karls-Universität Heidelberg, Heidelberg; (^b)Physikalisches Institut, Ruprecht-Karls-Universität Heidelberg, Heidelberg; Germany.
- ⁶²(^a)Department of Physics, Chinese University of Hong Kong, Shatin, N.T., Hong Kong; (^b)Department of Physics, University of Hong Kong, Hong Kong; (^c)Department of Physics and Institute for Advanced Study, Hong Kong University of Science and Technology, Clear Water Bay, Kowloon, Hong Kong; China.
- ⁶³Department of Physics, National Tsing Hua University, Hsinchu; Taiwan.
- ⁶⁴IJCLab, Université Paris-Saclay, CNRS/IN2P3, 91405, Orsay; France.
- ⁶⁵Department of Physics, Indiana University, Bloomington IN; United States of America.
- ⁶⁶(^a)INFN Gruppo Collegato di Udine, Sezione di Trieste, Udine; (^b)ICTP, Trieste; (^c)Dipartimento Politecnico di Ingegneria e Architettura, Università di Udine, Udine; Italy.
- ⁶⁷(^a)INFN Sezione di Lecce; (^b)Dipartimento di Matematica e Fisica, Università del Salento, Lecce; Italy.
- ⁶⁸(^a)INFN Sezione di Milano; (^b)Dipartimento di Fisica, Università di Milano, Milano; Italy.
- ⁶⁹(^a)INFN Sezione di Napoli; (^b)Dipartimento di Fisica, Università di Napoli, Napoli; Italy.
- ⁷⁰(^a)INFN Sezione di Pavia; (^b)Dipartimento di Fisica, Università di Pavia, Pavia; Italy.
- ⁷¹(^a)INFN Sezione di Pisa; (^b)Dipartimento di Fisica E. Fermi, Università di Pisa, Pisa; Italy.
- ⁷²(^a)INFN Sezione di Roma; (^b)Dipartimento di Fisica, Sapienza Università di Roma, Roma; Italy.

- ^{73(a)}INFN Sezione di Roma Tor Vergata;^(b)Dipartimento di Fisica, Università di Roma Tor Vergata, Roma; Italy.
- ^{74(a)}INFN Sezione di Roma Tre;^(b)Dipartimento di Matematica e Fisica, Università Roma Tre, Roma; Italy.
- ^{75(a)}INFN-TIFPA;^(b)Università degli Studi di Trento, Trento; Italy.
- ⁷⁶Universität Innsbruck, Department of Astro and Particle Physics, Innsbruck; Austria.
- ⁷⁷University of Iowa, Iowa City IA; United States of America.
- ⁷⁸Department of Physics and Astronomy, Iowa State University, Ames IA; United States of America.
- ^{79(a)}Departamento de Engenharia Elétrica, Universidade Federal de Juiz de Fora (UFJF), Juiz de Fora;^(b)Universidade Federal do Rio De Janeiro COPPE/EE/IF, Rio de Janeiro;^(c)Universidade Federal de São João del Rei (UFSJ), São João del Rei;^(d)Instituto de Física, Universidade de São Paulo, São Paulo; Brazil.
- ⁸⁰KEK, High Energy Accelerator Research Organization, Tsukuba; Japan.
- ⁸¹Graduate School of Science, Kobe University, Kobe; Japan.
- ^{82(a)}AGH University of Krakow, Faculty of Physics and Applied Computer Science, Krakow;^(b)Marian Smoluchowski Institute of Physics, Jagiellonian University, Krakow; Poland.
- ⁸³Institute of Nuclear Physics Polish Academy of Sciences, Krakow; Poland.
- ⁸⁴Faculty of Science, Kyoto University, Kyoto; Japan.
- ⁸⁵Kyoto University of Education, Kyoto; Japan.
- ⁸⁶Research Center for Advanced Particle Physics and Department of Physics, Kyushu University, Fukuoka ; Japan.
- ⁸⁷Instituto de Física La Plata, Universidad Nacional de La Plata and CONICET, La Plata; Argentina.
- ⁸⁸Physics Department, Lancaster University, Lancaster; United Kingdom.
- ⁸⁹Oliver Lodge Laboratory, University of Liverpool, Liverpool; United Kingdom.
- ⁹⁰Department of Experimental Particle Physics, Jožef Stefan Institute and Department of Physics, University of Ljubljana, Ljubljana; Slovenia.
- ⁹¹School of Physics and Astronomy, Queen Mary University of London, London; United Kingdom.
- ⁹²Department of Physics, Royal Holloway University of London, Egham; United Kingdom.
- ⁹³Department of Physics and Astronomy, University College London, London; United Kingdom.
- ⁹⁴Louisiana Tech University, Ruston LA; United States of America.
- ⁹⁵Fysiska institutionen, Lunds universitet, Lund; Sweden.
- ⁹⁶Centre de Calcul de l'Institut National de Physique Nucléaire et de Physique des Particules (IN2P3), Villeurbanne; France.
- ⁹⁷Departamento de Física Teórica C-15 and CIAFF, Universidad Autónoma de Madrid, Madrid; Spain.
- ⁹⁸Institut für Physik, Universität Mainz, Mainz; Germany.
- ⁹⁹School of Physics and Astronomy, University of Manchester, Manchester; United Kingdom.
- ¹⁰⁰CPPM, Aix-Marseille Université, CNRS/IN2P3, Marseille; France.
- ¹⁰¹Department of Physics, University of Massachusetts, Amherst MA; United States of America.
- ¹⁰²Department of Physics, McGill University, Montreal QC; Canada.
- ¹⁰³School of Physics, University of Melbourne, Victoria; Australia.
- ¹⁰⁴Department of Physics, University of Michigan, Ann Arbor MI; United States of America.
- ¹⁰⁵Department of Physics and Astronomy, Michigan State University, East Lansing MI; United States of America.
- ¹⁰⁶Group of Particle Physics, University of Montreal, Montreal QC; Canada.
- ¹⁰⁷Fakultät für Physik, Ludwig-Maximilians-Universität München, München; Germany.
- ¹⁰⁸Max-Planck-Institut für Physik (Werner-Heisenberg-Institut), München; Germany.
- ¹⁰⁹Graduate School of Science and Kobayashi-Maskawa Institute, Nagoya University, Nagoya; Japan.

- ¹¹⁰Department of Physics and Astronomy, University of New Mexico, Albuquerque NM; United States of America.
- ¹¹¹Institute for Mathematics, Astrophysics and Particle Physics, Radboud University/Nikhef, Nijmegen; Netherlands.
- ¹¹²Nikhef National Institute for Subatomic Physics and University of Amsterdam, Amsterdam; Netherlands.
- ¹¹³Department of Physics, Northern Illinois University, DeKalb IL; United States of America.
- ¹¹⁴Department of Physics, New York University, New York NY; United States of America.
- ¹¹⁵Ochanomizu University, Otsuka, Bunkyo-ku, Tokyo; Japan.
- ¹¹⁶Ohio State University, Columbus OH; United States of America.
- ¹¹⁷Homer L. Dodge Department of Physics and Astronomy, University of Oklahoma, Norman OK; United States of America.
- ¹¹⁸Department of Physics, Oklahoma State University, Stillwater OK; United States of America.
- ¹¹⁹Palacký University, Joint Laboratory of Optics, Olomouc; Czech Republic.
- ¹²⁰Institute for Fundamental Science, University of Oregon, Eugene, OR; United States of America.
- ¹²¹Graduate School of Science, Osaka University, Osaka; Japan.
- ¹²²Department of Physics, University of Oslo, Oslo; Norway.
- ¹²³Department of Physics, Oxford University, Oxford; United Kingdom.
- ¹²⁴LPNHE, Sorbonne Université, Université Paris Cité, CNRS/IN2P3, Paris; France.
- ¹²⁵Department of Physics, University of Pennsylvania, Philadelphia PA; United States of America.
- ¹²⁶Department of Physics and Astronomy, University of Pittsburgh, Pittsburgh PA; United States of America.
- ¹²⁷^(a)Laboratório de Instrumentação e Física Experimental de Partículas - LIP, Lisboa;^(b)Departamento de Física, Faculdade de Ciências, Universidade de Lisboa, Lisboa;^(c)Departamento de Física, Universidade de Coimbra, Coimbra;^(d)Centro de Física Nuclear da Universidade de Lisboa, Lisboa;^(e)Departamento de Física, Universidade do Minho, Braga;^(f)Departamento de Física Teórica y del Cosmos, Universidad de Granada, Granada (Spain);^(g)Dep Física and CEFITEC of Faculdade de Ciências e Tecnologia, Universidade Nova de Lisboa, Caparica;^(h)Departamento de Física, Instituto Superior Técnico, Universidade de Lisboa, Lisboa; Portugal.
- ¹²⁸Institute of Physics of the Czech Academy of Sciences, Prague; Czech Republic.
- ¹²⁹Czech Technical University in Prague, Prague; Czech Republic.
- ¹³⁰Charles University, Faculty of Mathematics and Physics, Prague; Czech Republic.
- ¹³¹Particle Physics Department, Rutherford Appleton Laboratory, Didcot; United Kingdom.
- ¹³²IRFU, CEA, Université Paris-Saclay, Gif-sur-Yvette; France.
- ¹³³Santa Cruz Institute for Particle Physics, University of California Santa Cruz, Santa Cruz CA; United States of America.
- ¹³⁴^(a)Departamento de Física, Pontificia Universidad Católica de Chile, Santiago;^(b)Millennium Institute for Subatomic physics at high energy frontier (SAPHIR), Santiago;^(c)Universidad Andres Bello, Department of Physics, Santiago;^(d)Instituto de Alta Investigación, Universidad de Tarapacá, Arica;^(e)Departamento de Física, Universidad Técnica Federico Santa María, Valparaíso; Chile.
- ¹³⁵Department of Physics, University of Washington, Seattle WA; United States of America.
- ¹³⁶Department of Physics and Astronomy, University of Sheffield, Sheffield; United Kingdom.
- ¹³⁷Department of Physics, Shinshu University, Nagano; Japan.
- ¹³⁸Department Physik, Universität Siegen, Siegen; Germany.
- ¹³⁹Department of Physics, Simon Fraser University, Burnaby BC; Canada.
- ¹⁴⁰SLAC National Accelerator Laboratory, Stanford CA; United States of America.
- ¹⁴¹Department of Physics, Royal Institute of Technology, Stockholm; Sweden.

- ¹⁴²Departments of Physics and Astronomy, Stony Brook University, Stony Brook NY; United States of America.
- ¹⁴³Department of Physics and Astronomy, University of Sussex, Brighton; United Kingdom.
- ¹⁴⁴School of Physics, University of Sydney, Sydney; Australia.
- ¹⁴⁵Institute of Physics, Academia Sinica, Taipei; Taiwan.
- ¹⁴⁶(^a) E. Andronikashvili Institute of Physics, Iv. Javakhishvili Tbilisi State University, Tbilisi; (^b) High Energy Physics Institute, Tbilisi State University, Tbilisi; Georgia.
- ¹⁴⁷Department of Physics, Technion, Israel Institute of Technology, Haifa; Israel.
- ¹⁴⁸Raymond and Beverly Sackler School of Physics and Astronomy, Tel Aviv University, Tel Aviv; Israel.
- ¹⁴⁹Department of Physics, Aristotle University of Thessaloniki, Thessaloniki; Greece.
- ¹⁵⁰International Center for Elementary Particle Physics and Department of Physics, University of Tokyo, Tokyo; Japan.
- ¹⁵¹Department of Physics, Tokyo Institute of Technology, Tokyo; Japan.
- ¹⁵²Department of Physics, University of Toronto, Toronto ON; Canada.
- ¹⁵³(^a) TRIUMF, Vancouver BC; (^b) Department of Physics and Astronomy, York University, Toronto ON; Canada.
- ¹⁵⁴Division of Physics and Tomonaga Center for the History of the Universe, Faculty of Pure and Applied Sciences, University of Tsukuba, Tsukuba; Japan.
- ¹⁵⁵Department of Physics and Astronomy, Tufts University, Medford MA; United States of America.
- ¹⁵⁶Department of Physics and Astronomy, University of California Irvine, Irvine CA; United States of America.
- ¹⁵⁷Department of Physics and Astronomy, University of Uppsala, Uppsala; Sweden.
- ¹⁵⁸Department of Physics, University of Illinois, Urbana IL; United States of America.
- ¹⁵⁹Instituto de Física Corpuscular (IFIC), Centro Mixto Universidad de Valencia - CSIC, Valencia; Spain.
- ¹⁶⁰Department of Physics, University of British Columbia, Vancouver BC; Canada.
- ¹⁶¹Department of Physics and Astronomy, University of Victoria, Victoria BC; Canada.
- ¹⁶²Fakultät für Physik und Astronomie, Julius-Maximilians-Universität Würzburg, Würzburg; Germany.
- ¹⁶³Department of Physics, University of Warwick, Coventry; United Kingdom.
- ¹⁶⁴Waseda University, Tokyo; Japan.
- ¹⁶⁵Department of Particle Physics and Astrophysics, Weizmann Institute of Science, Rehovot; Israel.
- ¹⁶⁶Department of Physics, University of Wisconsin, Madison WI; United States of America.
- ¹⁶⁷Fakultät für Mathematik und Naturwissenschaften, Fachgruppe Physik, Bergische Universität Wuppertal, Wuppertal; Germany.
- ¹⁶⁸Department of Physics, Yale University, New Haven CT; United States of America.
- ^a Also Affiliated with an institute covered by a cooperation agreement with CERN.
- ^b Also at Borough of Manhattan Community College, City University of New York, New York NY; United States of America.
- ^c Also at Bruno Kessler Foundation, Trento; Italy.
- ^d Also at Center for High Energy Physics, Peking University; China.
- ^e Also at Centro Studi e Ricerche Enrico Fermi; Italy.
- ^f Also at CERN, Geneva; Switzerland.
- ^g Also at CPPM, Aix-Marseille Université, CNRS/IN2P3, Marseille; France.
- ^h Also at Département de Physique Nucléaire et Corpusculaire, Université de Genève, Genève; Switzerland.
- ⁱ Also at Departament de Física de la Universitat Autònoma de Barcelona, Barcelona; Spain.
- ^j Also at Department of Financial and Management Engineering, University of the Aegean, Chios; Greece.
- ^k Also at Department of Physics and Astronomy, Michigan State University, East Lansing MI; United

States of America.

^l Also at Department of Physics and Astronomy, University of Louisville, Louisville, KY; United States of America.

^m Also at Department of Physics, Ben Gurion University of the Negev, Beer Sheva; Israel.

ⁿ Also at Department of Physics, California State University, East Bay; United States of America.

^o Also at Department of Physics, California State University, Fresno; United States of America.

^p Also at Department of Physics, California State University, Sacramento; United States of America.

^q Also at Department of Physics, King's College London, London; United Kingdom.

^r Also at Department of Physics, Stanford University, Stanford CA; United States of America.

^s Also at Department of Physics, University of Fribourg, Fribourg; Switzerland.

^t Also at Faculty of Physics, Sofia University, 'St. Kliment Ohridski', Sofia; Bulgaria.

^u Also at Giresun University, Faculty of Engineering, Giresun; Türkiye.

^v Also at Hellenic Open University, Patras; Greece.

^w Also at Institutio Catalana de Recerca i Estudis Avancats, ICREA, Barcelona; Spain.

^x Also at Institut für Experimentalphysik, Universität Hamburg, Hamburg; Germany.

^y Also at Institute for Nuclear Research and Nuclear Energy (INRNE) of the Bulgarian Academy of Sciences, Sofia; Bulgaria.

^z Also at Institute for Particle and Nuclear Physics, Wigner Research Centre for Physics, Budapest; Hungary.

^{aa} Also at Institute of Particle Physics (IPP); Canada.

^{ab} Also at Institute of Physics, Azerbaijan Academy of Sciences, Baku; Azerbaijan.

^{ac} Also at Institute of Theoretical Physics, Ilia State University, Tbilisi; Georgia.

^{ad} Also at Instituto de Fisica Teorica, IFT-UAM/CSIC, Madrid; Spain.

^{ae} Also at Istanbul University, Dept. of Physics, Istanbul; Türkiye.

^{af} Also at L2IT, Université de Toulouse, CNRS/IN2P3, UPS, Toulouse; France.

^{ag} Also at Physics Department, An-Najah National University, Nablus; Palestine.

^{ah} Also at Physikalisches Institut, Albert-Ludwigs-Universität Freiburg, Freiburg; Germany.

^{ai} Also at The City College of New York, New York NY; United States of America.

^{aj} Also at The Collaborative Innovation Center of Quantum Matter (CICQM), Beijing; China.

^{ak} Also at TRIUMF, Vancouver BC; Canada.

^{al} Also at Università di Napoli Parthenope, Napoli; Italy.

^{am} Also at University of Chinese Academy of Sciences (UCAS), Beijing; China.

^{an} Also at Yeditepe University, Physics Department, Istanbul; Türkiye.

* Deceased